Annu. Rev. Nucl. Part. Sci. 1998. 48:463–504

ELECTROWEAK STUDIES AT *Z* FACTORIES

Kaoru Hagiwara
Theory Group, KEK, Tsukuba, Ibaraki 305-0801, Japan and ICEPP, University of Tokyo, Tokyo 113-0033, Japan; e-mail: kaoru.hagiwara@kek.jp

KEY WORDS: standard model, radiative correction, Higgs mechanism

ABSTRACT

The Large Electron Positron collider LEP1 at CERN produced tens of millions of Z bosons, and the e^+e^- linear collider SLC at SLAC has produced Z bosons with its polarized e^- beam. Along with the measurements of the top-quark and W-boson masses at the Fermilab Tevatron $p\bar{p}$ collider, these Z-factory experiments have tested the standard electroweak theory with unprecedented precision. This chapter reviews the renormalizable gauge theory of the electroweak interactions and its quantum-level tests. Implications of the precision measurements are then studied within the standard model and its extentions.

CONTENTS

0163-8998/98/1201-0463$08.00

1. INTRODUCTION

Among the four known fundamental interactions of nature, the gravitational and the electromagnetic interactions are long-range, whereas the strong forces that bind nucleons in nuclei and the weak force that causes beta decays of nuclei are short-range. In quantum field theory, long-range interactions are mediated by the exchange of massless quanta, the graviton and the photon. Although the graviton has not been identified experimentally, the theory of the photon and charged particles, Quantum Electro Dynamics (QED), has been tested repeatedly at very high precision in many applications.

The short range of the remaining two interactions should be associated with an exchange of massive quanta. In fact, the range of the strong interaction among nucleons is associated with the mass of the π meson ($\approx$100 MeV), whereas that of the weak interactions is associated with the intermediate weak boson (W and Z) masses of slightly less than 100 GeV. This vast difference in range is not all that distinguishes the weak interactions from the strong interactions.

In the standard model of particle physics, hadrons (including π mesons) are composite objects made of quarks and gluons, and their masses are generated dynamically by the fundamental gauge theory of quarks and gluons known as Quantum Chromo Dynamics (QCD). Even though the color gauge symmetry based on the group SU(3) is unbroken, and hence its gauge bosons, gluons, are supposed to be massless, the dynamical phenomenon known as confinement allows only colorless composite states, hadrons, to be isolated as independent particles. Studies of deep-inelastic scattering of leptons and nucleons as well as lepton-pair or jet production in hadron and e^+e^- collisions have established that quarks and gluons exist and that their interactions are described by the color-SU(3) gauge theory, QCD.

According to the standard model, the intermediate weak bosons, W and Z, are the gauge bosons of the underlying $\mathrm{SU(2)_L} \otimes \mathrm{U(1)_Y}$ gauge symmetry, along with the photon, the gauge boson of the group $\mathrm{U(1)_{EM}}$. As is familiar for the photon in QED, gauge bosons should be massless, since the gauge symmetry forbids the appearance of an explicit gauge-boson mass term. However, a gauge boson can acquire a mass if the vacuum (the lowest-energy state of the theory) does not manifest the gauge symmetry. The mechanism is known as the spontaneous breakdown of gauge symmetry, or the Higgs mechanism (1). The heavy masses of W and Z result from the spontaneous breakdown of the $\mathrm{SU(2)_L} \otimes \mathrm{U(1)_Y}$ gauge symmetry down to $\mathrm{U(1)_{EM}}$ at a scale of 250 GeV. The origin of this spontaneous breakdown is not known; neither is the origin of masses and mixings of the quarks and leptons. The standard model assumes therefore the existence of at least one new force of nature, which could be called the real fifth force, that breaks gauge symmetry spontaneously and gives masses to quarks and leptons.

Historically, the weak interactions were expressed by Fermi as a product of two fermionic charged currents. Because the quark and lepton scattering amplitudes of the Fermi theory grow with energy, if the Fermi theory of the weak interactions is extrapolated to very high energies, the tree-level unitarity of the amplitudes is saturated at around 250 GeV (the Fermi scale), and they will start interacting nonperturbatively. As a consequence, the Fermi theory is not renormalizable, and it does not allow calculation of quantum corrections. In other words, weak interactions of each quark and lepton current should be measured separately to fix the coupling strength because the theory does not predict the relations among them. Experiments have found various universalities among different weak interaction strengths, such as the Cabibbo universality between the quark current and the lepton current, and a more fundamental theory of weak interactions has been anticipated.

Onset of the new strong interactions can be avoided if there are massive intermediate weak bosons below the Fermi scale. Massive vector-boson theory was studied extensively, especially after the $V - A$ structure of the weak charged currents was established, but it still suffers from severe ultraviolet divergences, for the vector-boson scattering amplitudes grow with energy and make the theory nonrenormalizable. The massive vector-boson theory thus loses its predictability. For example, the universality among weak currents can only be fixed by experiment, since no quantum corrections to the universality relations are calculable.

Weinberg (2) and Salam (3) proposed in the late 1960s that the theory may be renormalizable, and hence have predictive power, if the weak-boson masses are generated as a result of the spontaneous breakdown of the gauge symmetry $SU(2)_L \otimes U(1)_Y$ down to $U(1)_{EM}$—the group structure Glashow (4) proposed in 1961. The renormalizability of the theory was proved in 1971 by 't Hooft (5). The gauge symmetry gives the basis for the universality of various weak currents, and the renormalizability of the theory allows us to calculate quantum corrections in perturbation theory. The specific model of Weinberg and Salam gained phenomenological support during the 1970s: The Glashow-Iliopoulos-Maiani (GIM) (6) suppression mechanism for flavor-changing neutral currents was found in 1970, followed by the discovery of charmed quarks in 1974–1976. Neutral-current interactions were observed in 1973, and parity violation in the neutral-current electron-quark scattering was established by 1978. The $SU(2)_L \otimes U(1)_Y$ electroweak theory has been called the standard model since then. The W and Z bosons were found in 1983 at the masses expected in the theory.

What still remained to be tested was whether the observed W and Z bosons were indeed the gauge bosons of the broken $SU(2)_L \otimes U(1)_Y$ symmetry. In order to verify this, it is important to test the predictions of the theory at the

quantum level. This is because it is the predictability (renormalizability) of the model that distinguishes the Weinberg-Salam theory of the electroweak interactions from the massive–vector-boson models without the underlying gauge symmetry. Because the electroweak gauge-coupling constants are small, and because the quantum corrections are of the order of the square of the couplings, this requires high-precision measurements of the order of a few per mil accuracy. The first round of this test has been accomplished at two Z factories, LEP1 at CERN and SLC at SLAC, where millions of Z bosons are produced and their properties measured precisely.

In this chapter I summarize the overall achievements of these Z-factory experiments, as well as the other electroweak measurements, and describe the understanding of the nature of the weak interactions that has emerged as a consequence.

2. BASIC CONCEPTS OF THE ELECTROWEAK THEORY

2.1 *The Standard Model*

The standard model of the strong, electromagnetic, and weak interactions of elementary particles consists of four parts:

$$\mathcal{L}_{\rm SM} = \mathcal{L}_{\rm gauge} + \mathcal{L}_{\rm fermion} + \mathcal{L}_{\rm Higgs} + \mathcal{L}_{\rm Yukawa}. \tag{2.1.}$$

The first part consists of the $\mathrm{SU(3)_C} \otimes \mathrm{SU(2)_L} \otimes \mathrm{U(1)_Y}$ gauge bosons that mediate the strong and electroweak interactions:

$$\mathcal{L}_{\rm gauge} = -\frac{1}{4}F^a_{\mu\nu}F^{a\mu\nu} - \frac{1}{4}W^i_{\mu\nu}W^{i\mu\nu} - \frac{1}{4}B_{\mu\nu}B^{\mu\nu}, \tag{2.2.}$$

where

$$F^a_{\mu\nu} = \partial_\mu A^a_\nu - \partial_\nu A^a_\mu - g_s f^{abc} A^b_\mu A^c_\nu, \tag{2.3a.}$$

$$W^i_{\mu\nu} = \partial_\mu W^i_\nu - \partial_\nu W^i_\mu - g\epsilon^{ijk} W^j_\mu W^k_\nu, \tag{2.3b.}$$

$$B_{\mu\nu} = \partial_\mu B_\nu - \partial_\nu B_\mu. \tag{2.3c.}$$

Here $A^a_\mu(x)$ $(a = 1, \ldots, 8)$ are the gluons; $W^i_\mu(x)$ $(i = 1, 2, 3)$ and $B_\mu(x)$ are the electroweak bosons, which will be observed as the weak bosons $(W^\pm, Z)$ and the photon after the electroweak gauge symmetry $\mathrm{SU(2)_L} \otimes \mathrm{U(1)_Y}$ is broken down to $\mathrm{U(1)_{EM}}$. The coupling constants are g_s and g, and f^{abc} and ϵ^{ijk} are the structure constants of the gauge groups $\mathrm{SU(3)_C}$ and $\mathrm{SU(2)_L}$, respectively.

The second term consists of quarks and leptons and their interactions with the gauge bosons:

$$\mathcal{L}_{\rm fermion} = \sum_{f=Q,u_R,d_R,L,\ell_R} i\bar{\psi}_f D_\mu \gamma^\mu \psi_f, \tag{2.4.}$$

where $Q = (u_L, d_L)^T$ and $L = (\nu_L, \ell_L)^T$ are the $SU(2)_L$ doublets of left-handed quarks and leptons. All the right-handed quarks and leptons are $SU(2)_L$ singlets. The quarks Q, u_R, and d_R are $SU(3)_C$ color triplets, and the leptons L and ℓ_R are color singlets. In fact, three generations of these five types of fermions have been observed, and hence the summation is over the generation index as well. The interactions of quarks and leptons with the gauge bosons are dictated by the covariant derivative,

$$D_\mu = \partial_\mu + ig_s T^a A^a_\mu(x) + igT^i W^i_\mu(x) + ig' Y B_\mu(x), \qquad 2.5.$$

where g_s, g, and g' are the $SU(3)_C$ (strong), $SU(2)_L$, and $U(1)_Y$ (hypercharge) gauge couplings, respectively. The generators of the $SU(3)_C$ and $SU(2)_L$ groups are T^a $(a = 1, \ldots, 8)$ and T^i $(i = 1, 2, 3)$. For the $SU(2)_L$ doublets (left-handed quarks and leptons), T^i is one-half times the Pauli isospin matrices, $T^i = \sigma^i/2$. The hypercharge Y of quarks and leptons is $(1/6, 2/3, -1/3, -1/2, -1)$ for (Q, u_R, d_R, L, ℓ_R).

The Lagrangian density $\mathcal{L}_{SM}$ (2.1) is determined by two principles: (*a*) The interactions are invariant under gauge transformations. (*b*) Terms with energy dimension greater than four are suppressed. The gauge transformation is the phase transformation of the fields that depend on the spacetime point (x):

$$\psi_f(x) \to U(x)\psi_f(x), \qquad 2.6.$$

where the unitary matrix $U(x)$ is

$$U(x) = \exp(iT^a\theta^a(x) + iT^i\theta^i(x) + iY\theta(x)). \qquad 2.7.$$

The gauge bosons transform such that the covariant derivative term (Equation 2.5) transforms covariantly under the gauge transformation:

$$D_\mu \to U(x) D_\mu U(x)^\dagger. \qquad 2.8.$$

The gauge invariance of $\mathcal{L}_{\text{fermion}}$ (Equation 2.4) is then obvious. That of $\mathcal{L}_{\text{gauge}}$ can be seen by noticing that the gauge-boson tensors (Equation 2.3) are obtained from the commutator $[D_\mu, D_\nu]$, which transforms covariantly, $[D_\mu, D_\nu] \to U(x)[D_\mu, D_\nu]U(x)^\dagger$, and that the trace of their Lorentz-invariant contraction, $Tr\{[D_\mu, D_\nu][D^\mu, D^\nu]\}$, is invariant. The gauge invariance thus tells us that the gauge bosons appear in the Lagrangian only in association with the derivative of the fields. The two most important consequences of the gauge invariance then follow:

1. Gauge bosons interact with all fields with a unique gauge-coupling constant for each gauge group.

2. Gauge bosons are massless.

In addition, since the left-handed and the right-handed components of quarks and leptons transform differently under $SU(2)_L$,

3. Quarks and leptons are massless.

The first rule means, for example, that all quarks interact with gluons with the same coupling strength and that all left-handed fermions (whether quarks or leptons) interact with W^i bosons the same way. Not only their interactions with quarks and leptons but also their self-interactions in $\mathcal{L}_{\text{gauge}}$ are forced to have the universal strength as can be seen from Equation 2.3. The second rule is found not to contradict with observation for the $SU(3)_C$ gauge bosons (gluons) because of the confinement of quarks and gluons. However, it clearly disagrees with the observation that the W and Z bosons are massive. Naive introduction of W and Z mass terms in the Lagrangian breaks gauge invariance in such a way that higher-dimensional terms in the Lagrangian are generated and the renormalizability, or predictive power, of the theory is lost.

In the standard model, the weak-boson masses are generated by the spontaneous breakdown of the $SU(2)_L \otimes U(1)_Y$ electroweak gauge symmetry. This is done in the Higgs sector:

$$\mathcal{L}_{\text{Higgs}} = \sum_i (D_\mu H_i)^\dagger (D^\mu H_i) - V(H_i), \qquad 2.9.$$

where the scalar fields H_i are generically called the Higgs bosons. They interact through the potential $V(H_i)$, which is minimized when some components of H_i take nonzero constant values. If the vacuum expectation values (vevs) of the Higgs bosons break the electroweak symmetry but preserve the electromagnetic symmetry, the $SU(2)_L \otimes U(1)_Y$ symmetry is spontaneously broken down to the $U(1)_{EM}$ symmetry. Three of the four electroweak gauge bosons then acquire masses to become the observed $W^\pm$ and Z bosons, and the photon appears as the massless gauge boson of the remaining $U(1)_{EM}$ gauge symmetry. The observed gauge bosons are related to the original fields in $\mathcal{L}_{\text{gauge}}$ as $W_\mu^\pm = 1/\sqrt{2}(W_\mu^1 \mp i W_\mu^2)$ and

$$\begin{pmatrix} W_\mu^3 \\ B_\mu \end{pmatrix} = \begin{pmatrix} c_W & s_W \\ -s_W & c_W \end{pmatrix} \begin{pmatrix} Z_\mu \\ A_\mu \end{pmatrix}, \qquad 2.10.$$

where A_μ denotes the photon field, $s_W = \sin\theta_W$, and $c_W = \cos\theta_W$. The electroweak mixing angle θ_W plays an essential role in the following analysis. In terms of the physical electroweak bosons, the electroweak part of the covariant

derivative (Equation 2.4) can be written as

$$D_\mu = \partial_\mu + i\frac{g}{\sqrt{2}}(T^+W_\mu^+ + T^-W_\mu^-) + ig_Z(T^3 - s_W^2 Q)Z_\mu + ieQA_\mu, \qquad 2.11.$$

where $T^\pm = T^1 \pm iT^2$; T^3 gives the weak isospin of the quarks, leptons, and Higgs multiplets; and $Q = T^3 + Y$ gives the electric charge in units of the positron charge. The gauge coupling constants are related by the electroweak mixing angle as $e = gs_W = g_Z c_W s_W$. In generating the weak-boson masses, the mechanism of spontaneous gauge-symmetry breakdown has the following advantages: (*a*) The universality of all the electroweak interactions is preserved, since the gauge invariance of all the interactions is preserved. (*b*) The theory remains renormalizable, and all experimental observables can be calculated accurately in perturbation theory in terms of a finite number of inputs.

If the Higgs boson H_i with weak isospin T_i and hypercharge Y_i obtains the vev, $v_i/\sqrt{2}$, in its $Q = T_i^3 + Y_i = 0$ component, then from Equations 2.9 and 2.11, the weak bosons obtain masses as follows:

$$m_W^2 = \frac{g^2}{2}\sum_i [T_i(T_i+1) - (Y_i)^2]v_i^2, \qquad 2.12a.$$

$$m_Z^2 = g_Z^2 \sum_i [(Y_i)^2]v_i^2. \qquad 2.12b.$$

Because the ratio g^2/m_W^2 is proportional to the muon decay constant G_F, we have the following sum rule:

$$2\sum_i [T_i(T_i+1) - (Y_i)^2]v_i^2 = v^2 \equiv \frac{1}{\sqrt{2}G_F} \approx (246\ \text{GeV})^2. \qquad 2.13.$$

Finally the quark and lepton masses are generated by their gauge-invariant interactions with the Higgs bosons in $\mathcal{L}_{\text{Yukawa}}$:

$$\mathcal{L}_{\text{Yukawa}} = \sum_{ij} f_{ij}^u H_u^* \overline{Q}_i u_{jR} + f_{ij}^d H_d^* \overline{Q}_i d_{jR} + f_{ij}^l H_d^* \overline{L}_i l_{jR} + (h.c.), \qquad 2.14.$$

where i and j are generation indices. Because the left-handed fermions are doublets and the right-handed ones are singlets, SU(2)_L doublet Higgs bosons are necessary for gauge-invariant Yukawa interactions. In the above example, we introduced two Higgs bosons, $H_u(Y = 1/2)$ and $H_d(Y = -1/2)$. By denoting their vevs as $v_u/\sqrt{2}$ and $v_d/\sqrt{2}$, respectively, the quark and lepton mass matrices are obtained as $M_{ij}^u = f_{ij}^u v_u/\sqrt{2}$, $M_{ij}^d = f_{ij}^d v_d/\sqrt{2}$, and $M_{ij}^\ell = f_{ij}^\ell v_d/\sqrt{2}$. In the minimal standard model, the field H_u is obtained as the charge conjugation of the field H_d, as $H_u = i\sigma^2 H_d^*$. In the minimal supersymmetric standard

model (MSSM), the two are distinct fields. In both models, we assume that only those Higgs bosons necessary to generate the quark and lepton masses also give masses to the weak bosons. In this class of models where the spontaneous electroweak symmetry breaking is caused only by the Higgs doublets, there is one distinct relationship among the weak-boson masses and the gauge couplings (7):

$$\rho = \frac{g_Z^2/m_Z^2}{g^2/m_W^2} = 1. \qquad 2.15.$$

The strength of the neutral-current interactions is the same as that of the charged-current interactions. One can easily verify the identity (Equation 2.15) by inserting $T_i = |Y_i| = 1/2$ in Equation 2.12. This is a consequence of the accidental SU(2) symmetry (8) that survives after the spontaneous symmetry breaking in the models with doublet Higgs bosons only. It is a combination of the $SU(2)_L$ gauge symmetry and the additional global SU(2) symmetry that mixes H_u and H_d. In both the minimal standard model and the MSSM, the large splitting between the top-quark and the bottom-quark masses violates the global SU(2) symmetry. The relation (Equation 2.15) is thus expected to be violated by radiative corrections even in models with only doublet Higgs bosons.

In general, the ρ parameter can have an arbitrary value:

$$1 - \frac{1}{\rho} = \frac{2\sum_i [T_i(T_i+1) - 3(Y_i)^2]v_i^2}{v^2}, \qquad 2.16.$$

from Equations 2.12 and 2.13. The tree-level ρ parameter can be bigger or smaller than unity, or can still be unity if a cancellation takes place among nondoublet Higgs-boson vevs.

2.2 *Quantum Corrections and Precision Measurements*

The standard model of the elementary particles is a renormalizable quantum field theory that allows us to predict the cross sections in perturbation theory to a desired accuracy. Because the electroweak gauge-coupling constants are relatively small, one-loop quantum corrections are usually sufficient to obtain the desired accuracy. Two- and three-loop corrections are included when corrections involve the strong-coupling constant and/or the top-quark Yukawa coupling. As inputs, the calculation requires the quark and lepton masses; the Higgs-boson mass in the minimal standard model; m_W and m_Z; and the three gauge-coupling constants, $\alpha_s = g_s^2/4\pi$, $\alpha_W = g^2/4\pi$, and $\alpha = e^2/4\pi$. Schematically, the standard-model Lagrangian has the following parameters:

$$\overbrace{g_s, g, g'}^{\mathcal{L}_{\text{gauge}}+\mathcal{L}_{\text{fermion}}} \quad \overbrace{m_W, m_Z, m_H, \ldots}^{\mathcal{L}_{\text{Higgs}}} \quad \overbrace{m_t, \ldots,}^{\mathcal{L}_{\text{Yukawa}}} \qquad 2.17.$$

where all the quark and lepton masses except for m_t are suppressed, and ... denotes unknown parameters in the Higgs and Yukawa sectors. In models with Higgs doublets only, the tree-level identity (Equation 2.15) implies that only one gauge-boson mass, m_W or m_Z, is needed as the input weak-boson mass scale. The other mass can be calculated accurately in terms of the remaining parameters of the theory. In the minimal standard model with only one Higgs doublet, all the couplings in the Yukawa sector are essentially determined by the observed quark and lepton masses and the Cabibbo-Kobayashi-Maskawa quark-flavor mixing matrix elements.

In the electroweak sector, the three basic parameters, the two gauge couplings and the scale of the spontaneous symmetry breaking (v^2 or m_W^2/g^2), can be constrained by the three most accurately measured quantities: the fine structure constant α, the muon decay constant G_F, and the Z-boson mass m_Z. Their observed values are (9)

$$1/\alpha = 137.0359895(61), \qquad 2.18a.$$

$$G_F = 1.16639(2) \times 10^{-5}\ \mathrm{GeV}^{-2}, \qquad 2.18b.$$

$$m_Z = 91.1867(20)\ \mathrm{GeV}. \qquad 2.18c.$$

The 1-σ uncertainties in the last digits are given in the parentheses: the fractional uncertainties are 4×10^{-8} for α, 2×10^{-5} for both G_F and m_Z. These uncertainties are so small that we can safely neglect them in the following analysis. In fact, the measurement of m_Z with an accuracy comparable to that of the muon decay constant is one of the most important achievements of the LEP1 experiments.

Unfortunately, the electroweak radiative corrections depend more directly on the running QED coupling constant at the m_Z scale, $\bar{\alpha}(m_Z^2)$, than on the precisely measured fine structure constant, $\alpha = \bar{\alpha}(0)$. This is mainly because the typical energy scale (or the inverse of the distance scale) of the electroweak phenomena studied is the weak-boson mass scale rather than the electron mass scale below which the fine structure constant is measured. This is true even for the muon decay constant, since the effective range of the weak interactions is determined by the weak-boson mass rather than the muon mass. We should therefore use the effective gauge-coupling constants at the weak-boson mass scale as the expansion parameters in order to achieve reliable perturbation-theory predictions for the electroweak observable.

The running QED coupling at the weak-boson mass scale can be calculated accurately in QED by using the renormalization group method (10) to sum up vacuum-polarization corrections. The only obstacle is in the evaluation of the light-quark contribution to the photon vacuum-polarization function at low energies ($|q^2| \lesssim$ a few GeV^2), where nonperturbative QCD effects are essential.

At low energies, the data from $e^+e^- \to$ hadrons are used to evaluate the imaginary part of the vacuum-polarization function, and its real part is determined using the dispersion relation. Because the analysis necessarily requires interpolation between the available data points, several estimates are obtained from essentially the same input data sets. Among the most recent estimates (11–16), we adopt (13, 14)

$$1/\bar{\alpha}\left(m_Z^2\right) = 128.75 \pm 0.09 \qquad 2.19.$$

as the standard reference value, since the estimate is least model-dependent and hence most conservative. We note here that the effective QED coupling contains both the top-quark and the W-boson contributions (17), whereas the running coupling constant with fermions only, $\alpha(q^2)_{\rm f}$, and that with light-fermions only, $\alpha(q^2)_{\rm lf}$, are often quoted. They are related as

$$1/\alpha\left(m_Z^2\right)_{\rm lf} = 1/\alpha\left(m_Z^2\right)_{\rm f} - 0.01 = 1/\bar{\alpha}\left(m_Z^2\right) + 0.14 \qquad 2.20.$$

rather accurately for $m_t \sim 175$ GeV and $m_W \sim 80$ GeV. The barred effective charges (17) allow us to relate all the electroweak vacuum-polarization corrections compactly, and they remain as effective coupling constants even at energies far above the weak scale $|q^2| \gg m_Z^2$ (18, 17).

Some alternative estimates of $\bar{\alpha}(m_Z^2)$ assume, for example, the smoothness of the e^+e^- hadroproduction cross section (12) in order to take advantage of the smaller experimental uncertainty in the energy dependence of the cross section as compared to its normalization. Some estimates adopt the perturbative QCD prediction to constrain the normalization of low-energy data down to ~3 GeV (11), or use the perturbative QCD formulae down to m_τ (15, 16). To show the dependence of the electroweak observable to the present estimates of $\bar{\alpha}(m_Z^2)$, and to study the implications of its future improvements, we introduce the parameter (17)

$$\delta_\alpha \equiv 1/\bar{\alpha}\left(m_Z^2\right) - 128.72, \qquad 2.21.$$

in terms of which the standard estimate (2.19) and its alternatives are

$$\delta_\alpha = 0.03 \pm 0.09 \quad \text{[EJ] (13)}, \qquad 2.22a.$$

$$\delta_\alpha = 0.12 \pm 0.06 \quad \text{[MZ] (11)}, \qquad 2.22b.$$

$$\delta_\alpha = 0.07 \pm 0.04 \quad \text{[DH] (15)}. \qquad 2.22c.$$

By comparing the sensitivity of the electroweak observables to these three estimates, we can gauge the impacts of future improvements in low-energy e^+e^- hadroproduction measurements.

The present fractional uncertainty (13, 14) of the $\bar{\alpha}(m_Z^2)$ parameter is 7×10^{-4}, which is of the same order as the uncertainty in some of the most accurately

measured electroweak observables at the Z^0 factories and the Tevatron. It is therefore essential to keep track of the uncertainty in δ_α throughout the calculation.

In order to organize various electroweak radiative corrections, it is convenient to introduce four effective running couplings that contain all the gauge-boson propagator corrections in the $\mathrm{SU(2)_L} \otimes \mathrm{U(1)_Y}$ gauge theories. Associated with the four types of the gauge-boson propagators, we define (17)

$$\bar{e}^2(q^2) \equiv \hat{e}^2(\mu)\left[1 - \overline{\Pi}^{\gamma\gamma}_{T,\gamma}(q^2)\right], \qquad 2.23a.$$

$$\bar{s}^2(q^2) \equiv \hat{s}^2(\mu)\left[1 + \frac{\hat{c}(\mu)}{\hat{s}(\mu)}\overline{\Pi}^{\gamma Z}_{T,\gamma}(q^2)\right], \qquad 2.23b.$$

$$\bar{g}^2_Z(q^2) \equiv \hat{g}^2_Z(\mu)\left[1 - \overline{\Pi}^{ZZ}_{T,Z}(q^2)\right], \quad \text{and} \qquad 2.23c.$$

$$\bar{g}^2_W(q^2) \equiv \hat{g}^2(\mu)\left[1 - \overline{\Pi}^{WW}_{T,W}(q^2)\right], \qquad 2.23d.$$

where $\overline{\Pi}^{AB}_{T,V}(q^2) \equiv [\overline{\Pi}^{AB}_T(q^2) - \overline{\Pi}^{AB}_T(m_V^2)]/(q^2 - m_V^2)$ are the propagator correction factors that appear in the S-matrix elements after the weak-boson mass renormalization is performed, and $\hat{e} \equiv \hat{g}\hat{s} \equiv \hat{g}_Z\hat{s}\hat{c}$ are the $\overline{\mathrm{MS}}$ couplings. The overlines denote the inclusion of pinch terms (19), which makes $\overline{\Pi}^{\gamma Z}_{T,\gamma}(0) = 0$ automatic and also makes the effective couplings useful (17, 18, 20, 21) even at very high energies ($|q^2| \gg m_Z^2$).

In order to determine the two weak-boson masses and the four effective couplings at a given scale, six inputs are in general necessary. It is most convenient to choose three numerical inputs, $\bar{\alpha}(m_Z^2)$, G_F, and m_Z, and three parameters (22–26) that can be determined from experiments and are calculable in a wide class of electroweak models. Following the notation of Peskin & Takeuchi (22), we define (17)

$$\frac{\bar{s}^2(m_Z^2)\bar{c}^2(m_Z^2)}{\bar{\alpha}(m_Z^2)} - \frac{4\pi}{\bar{g}^2_Z(0)} \equiv \frac{S}{4}, \qquad 2.24a.$$

$$\frac{\bar{s}^2(m_Z^2)}{\bar{\alpha}(m_Z^2)} - \frac{4\pi}{\bar{g}^2_W(0)} \equiv \frac{S+U}{4}, \qquad 2.24b.$$

$$1 - \frac{\bar{g}^2_W(0)}{m_W^2}\frac{m_Z^2}{\bar{g}^2_Z(0)} \equiv \alpha T, \qquad 2.24c.$$

where $\bar{c}^2 = 1 - \bar{s}^2$. With this definition, the S, T, U parameters receive contributions from both the standard-model radiative effects and new physics.

For a given electroweak model we can calculate the S, T, U parameters (T is a free parameter in models without a custodial SU(2) symmetry), and the

effective couplings are then fixed by the following identities (17):

$$\frac{1}{\bar{g}_Z^2(0)} = \frac{1+\bar{\delta}_G - \alpha T}{4\sqrt{2}\, G_F m_Z^2}, \tag{2.25a.}$$

$$\bar{s}^2\left(m_Z^2\right) = \frac{1}{2} - \sqrt{\frac{1}{4} - \bar{\alpha}\left(m_Z^2\right)\left(\frac{4\pi}{\bar{g}_Z^2(0)} + \frac{S}{4}\right)}, \tag{2.25b.}$$

$$\frac{4\pi}{\bar{g}_W^2(0)} = \frac{\bar{s}^2\left(m_Z^2\right)}{\bar{\alpha}^2\left(m_Z^2\right)} - \frac{1}{4}(S+U). \tag{2.25c.}$$

Here $\bar{\delta}_G$ is the vertex and box correction to the muon lifetime (27) after subtracting the pinch term (17):

$$G_F = \frac{\bar{g}_W^2(0) + \hat{g}^2\bar{\delta}_G}{4\sqrt{2}\, m_W^2}. \tag{2.26.}$$

In the standard model, $\bar{\delta}_G = 0.0055$ (17).

It is clear from the above identities that once we know T and $\bar{\delta}_G$ in a given model we can predict $\bar{g}_Z^2(0)$ from Equation 2.25a. Then, knowing S and $\bar{\alpha}(m_Z^2)$, we can calculate $\bar{s}^2(m_Z^2)$ from Equation 2.25b, and knowing U we can calculate $\bar{g}_W^2(0)$ from Equation 2.25c. The three effective couplings are thus fixed at one q^2 point. The difference between $\bar{\alpha}(m_Z^2)$ and the fine structure constant α has been evaluated and parameterized by δ_α in Equations 2.21 and 2.22. The difference

$$\frac{\bar{s}^2(0)}{\alpha} - \frac{\bar{s}^2\left(m_Z^2\right)}{\bar{\alpha}\left(m_Z^2\right)} \approx 3.09 - \frac{\delta_\alpha}{2} \tag{2.27.}$$

depends on the same δ_α (17), and the difference

$$\frac{4\pi}{\bar{g}_Z^2\left(m_Z^2\right)} - \frac{4\pi}{\bar{g}_Z^2(0)} \approx -0.299 + 0.031\log\left[1 + \left(\frac{26\ \text{GeV}}{m_H}\right)^2\right] \tag{2.28.}$$

depends on m_H when $m_H \lesssim m_Z$ (17, 28). For the following analysis, it is convenient to expand the effective couplings about the reference standard-model predictions at $m_t = 175$ GeV, $m_H = 100$ GeV, and $\delta_\alpha = 0.03$ (Equation 2.22a):

$$\bar{g}_Z^2\left(m_Z^2\right) = 0.55635 + \Delta\bar{g}_Z^2, \tag{2.29a.}$$

$$\bar{s}^2\left(m_Z^2\right) = 0.23035 + \Delta\bar{s}^2, \tag{2.29b.}$$

$$m_W[\text{GeV}] = 80.402 + \Delta m_W, \tag{2.29c.}$$

where m_W replaces $\overline{g}_W^2(0)$ via Equation 2.26. The shifts from the reference values are expressed as

$$\Delta\overline{g}_Z^2 = 0.00412\Delta T + 0.00005[1 - (100\ \text{GeV}/m_H)^2], \qquad 2.30a.$$

$$\Delta\overline{s}^2 = 0.00360\Delta S - 0.00241\Delta T - 0.00023x_\alpha, \qquad 2.30b.$$

$$\Delta m_W[\text{GeV}] = -0.288\Delta S + 0.418\Delta T + 0.337\Delta U + 0.012x_\alpha, \qquad 2.30c.$$

where

$$\Delta S = S + 0.233 = \Delta S_{\text{SM}} + S_{\text{new}}, \qquad 2.31a.$$

$$\Delta T = T - 0.879 = \Delta T_{\text{SM}} + T_{\text{new}}, \qquad 2.31b.$$

$$\Delta U = U - 0.362 = \Delta U_{\text{SM}} + U_{\text{new}}. \qquad 2.31c.$$

The standard-model contributions are parameterized as (28)

$$\Delta S_{\text{SM}} = -0.007x_t + 0.091x_H - 0.010x_H^2, \qquad 2.32a.$$

$$\Delta T_{\text{SM}} = (0.130 - 0.003x_H)x_t + 0.003x_t^2 - 0.079x_H - 0.028x_H^2 + 0.0026x_H^3, \qquad 2.32b.$$

$$\Delta U_{\text{SM}} = 0.022x_t - 0.002x_H, \qquad 2.32c.$$

in terms of the variables

$$x_t = \frac{m_t - 175\ \text{GeV}}{10\ \text{GeV}}, \quad x_H = \ln\frac{m_H}{100\ \text{GeV}}, \quad x_\alpha = \frac{\delta_\alpha - 0.03}{0.09}, \qquad 2.33.$$

which vanish at the reference point. The above parameterizations are valid in the range $160 < m_t[\text{GeV}] < 185$ and $60 < m_H[\text{GeV}] < 1000$ and are useful in studying the implications of present and future electroweak measurements. Outside that region, especially at smaller m_H, more exact formulae should be used [see e.g. Appendix C of Hagiwara et al (17)].

Once the effective couplings $\overline{\alpha}(m_Z^2)$ and $\overline{s}^2(m_Z^2)$ are determined, the $\overline{\text{MS}}$ couplings can be calculated from their defining formulae, Equations 2.23a and 2.23b. In the standard model,

$$\frac{1}{\hat{\alpha}(m_Z)} = \frac{1}{\overline{\alpha}(m_Z^2)} - 0.88 + \frac{8}{9\pi}\left(1 + \frac{\alpha_s}{\pi}\right)\ln\frac{m_t}{m_Z}, \qquad 2.34a.$$

$$\frac{\hat{s}^2(m_Z)}{\hat{\alpha}(m_Z)} = \frac{\overline{s}^2(m_Z^2)}{\overline{\alpha}(m_Z^2)} - 0.11 + \frac{1}{3\pi}\left(1 + \frac{\alpha_s}{\pi}\right)\ln\frac{m_t}{m_Z}, \qquad 2.34b.$$

where $\hat{\alpha}(\mu) = \hat{e}^2(\mu)/4\pi$ and $\hat{s}^2(\mu)$ are the standard-model $\overline{\text{MS}}$ couplings, and we include only the order α_s two-loop effects. These $\overline{\text{MS}}$ couplings are then used

to test the grand unification of the three gauge couplings. By dropping terms proportional to $\ln(m_t/m_Z)$ of Equation 2.34, one obtains the $\overline{\rm MS}$ couplings of the effective theory without the top quark, just like the standard definition of the QCD coupling, $\hat{\alpha}_s(m_Z) \equiv \alpha_s(m_Z)_{\overline{\rm MS}}$. For our reference standard-model parameters, $m_t = 175$ GeV, $m_H = 100$ GeV, and $1/\bar{\alpha}(m_Z^2) = 128.75$, we find $1/\hat{\alpha}(m_Z) = 127.87$ and $\hat{\rm s}^2(m_Z) = 0.23108$ for the effective theory couplings. These $\overline{\rm MS}$ couplings can be used as expansion parameters of the perturbative calculation, and the dependences of the predictions on their magnitude (e.g. from other choices of the scale μ, such as $\mu = m_Z/2$) measure the uncertainty due to higher-order corrections. Uncertainties owing to these and other higher-order corrections have been evaluated and found to be small (29), and recent work (30) has reduced them significantly further.

The above parameterizations and the following analyses are all based on the theoretical formulae presented in Hagiwara et al (17). Among the potentially relevant recent improvements to the standard-model radiative corrections are the three-loop (order α_s^2) QCD calculation of the T parameter (31), the two-loop (order $g^4 m_t^2$) contribution to the relation between the weak-boson masses and G_F (30), and two-loop nonfactorizable QCD and electroweak corrections to the hadronic Z-boson decay rates (32). Although we do not include these recent improvements, we find generally good agreement with the results of the LEP electroweak working group (33).

3. ELECTROWEAK MEASUREMENTS

3.1 *Observables at Z Factories*

All the precision experiments sensitive to electroweak physics at the one-loop level so far are concerned with processes involving external fermions, that is, leptons or quarks (excluding top quarks), whose masses can safely be neglected in the correction terms as compared to the weak-boson masses. They are the Z-boson properties as measured at LEP1 and SLC, the neutral-current processes at low energies ($\ll m_Z$), the measurements of charged-current processes at low energies, and the measurements of the W mass at the Tevatron and LEP2. The relevant observables in these processes are then expressed in terms of the S-matrix elements of four external fermions, which form a scalar product of two chirality-conserving currents. All the information on electroweak physics is contained in the scalar amplitudes that multiply these current-current products.

For example, consider the S-matrix element responsible for the generic four-fermion neutral-current process $ij \to ij$ (or any one of its crossed channels), e.g. $e^+e^- \to f\bar{f}$ or $\nu_\mu q \to \nu_\mu q$. The matrix element has the form

$$T_{ij} = M_{ij}\, J_i \cdot J_j, \qquad 3.1.$$

where J_i^μ and J_j^μ denote currents without coupling factors, that is, $J_i^\mu = \bar{\psi}_f \gamma^\mu P_\alpha \psi_f$ for $i = f_\alpha$, with $P_\alpha = (1 + \alpha\gamma_5)/2$ where $\alpha = \pm 1$ are the chiral projectors. [This chapter uses the notation $P_+ = P_R$, $P_- = P_L$, $f_+ = f_R$, $f_- = f_L$, $\overline{f_L} = (\bar{f})_R$, and $\overline{f_R} = (\bar{f})_L$.] In the massless fermion limit, the current products take very simple forms, e.g. for $e_\alpha \overline{e_\alpha} \to f_\beta \overline{f_\beta}$,

$$J_{e_\alpha} \cdot J_{f_\beta} = \sqrt{s}(1 + \alpha\beta \cos\theta), \qquad 3.2.$$

where $\sqrt{s}$ is the e^+e^- energy and θ is the scattering angle between the e^- and the f momenta in the e^+e^- collision center-of-mass (c.m.) frame. All radiative effects that interfere with the tree-level standard-model amplitudes can be cast in the above form as long as terms of order m_f^2/m_Z^2 in the one-loop amplitudes are neglected (m_f denoting the external fermion mass). The one-loop corrections then appear in the scalar amplitudes M_{ij}, which depend on the flavor and chirality of the currents and on the invariant momentum transfers s and t of the process.

In neutral-current amplitudes, the photonic corrections attached only to the external fermion lines are $U(1)_{EM}$ gauge–invariant by themselves (34). Therefore, finite and gauge-invariant amplitudes can be obtained by excluding all the external photonic corrections. The generic neutral-current amplitude M_{ij} of (3.1) then takes the following form at one-loop order (17):

$$\begin{aligned} M_{ij} = & \frac{Q_i Q_j}{s}\left[\bar{e}^2(s) + \hat{e}^2\left(\Gamma_1^i + \Gamma_1^j\right)(s) - i\hat{e}^2\Delta_{\gamma\gamma}(s)\right] \\ & + \hat{e}^2\left[(Q_i I_{3j})\frac{\overline{\Gamma}_2^j(s)}{s} + (I_{3i} Q_j)\frac{\overline{\Gamma}_2^i(s)}{s}\right] + \frac{1}{s - m_Z^2 + is\frac{\Gamma_Z}{m_Z}\theta(s)} \\ & \times \left\{(I_{3i} - Q_i\hat{s}^2)(I_{3j} - Q_j\hat{s}^2)\left[\bar{g}_Z^2(s) + \hat{g}_Z^2\left(\Gamma_1^i + \Gamma_1^j\right)(s)\right.\right. \\ & \left. - i\hat{g}_Z^2\Delta_{ZZ}(s)\right] + (I_{3i} - Q_i\hat{s}^2)\hat{g}_Z^2\left[I_{3j}\left(\hat{c}^2\overline{\Gamma}_2^j + \Gamma_3^j\right)(s)\right. \\ & \left. - Q_j(\bar{s}^2(s) - \hat{s}^2 + i\Delta_{\gamma Z}(s))\right] + (I_{3j} - Q_j\hat{s}^2)\hat{g}_Z^2\left[I_{3i}\left(\hat{c}^2\overline{\Gamma}_2^i + \Gamma_3^i\right)(s)\right. \\ & \left.\left. - Q_i(\bar{s}^2(s) - \hat{s}^2 + i\Delta_{\gamma Z}(s))\right]\right\} + B_{ij}(s,t). \qquad 3.3. \end{aligned}$$

Here Q_f and I_{3f_α} denote the electric charge and the third component of weak isospin, respectively, of fermion f_α. $\Gamma_k^{f_\alpha}, \overline{\Gamma}_k^{f_\alpha} (k = 1, 2, 3)$ are complex vertex functions that contain external fermion self-energy corrections, and the Δ_{AB} are the imaginary parts of the AB propagator corrections. The use of the running width in the Z-propagator factor makes Δ_{ZZ} very small at $s = m_Z^2$. The B_{ij} are the box functions, which are negligible near the Z pole. The explicit forms

of all these functions and their numerical values are found e.g. in Appendix A of Hagiwara et al (17).

The reduced amplitudes (Equation 3.3) contain all the information on the electroweak physics at the Z-boson mass scale and at shorter distances. Experiments are performed, however, at macroscopic distances, and the experimental observables are affected by physics at longer distances. This long-distance physics is dictated by the unbroken parts of the standard-model gauge interactions, QED and QCD. Fortunately, reliable calculation of the consequences of QED radiation effects is possible using perturbation theory. Perturbation theory is also useful for evaluating the QCD corrections down to a few-GeV scale, below which nonperturbative hadronization of quarks and gluons occurs. Although the hadronization effects are incalculable at present, they have been parameterized phenomenologically using Monte Carlo event generators that incorporate perturbative quark and gluon radiation down to a few-GeV scale and model the hadronization at lower scales. Detailed experimental studies on hadron jets at LEP1/SLC and experiments at lower energy have contributed to the tuning of those phenomenological models. Much effort has been devoted to improving the evaluation of long-distance effects for the Z-pole experiments (29, 34), since they play an essential role behind all the precision measurements.

Among the long-distance corrections, the corrections due to multiple emission of photons and e^+e^- pairs from the colliding e^+e^- beams have been evaluated with extra care because they affect the luminosity measurement and the effective energy scale probed by the experiments. Schematically, experiments at a given e^+e^- c.m. energy $\sqrt{s}$ observe the convolution of the cross section calculated from the short-distance amplitudes (Equation 3.1) over the effective collision energy $\sqrt{\hat{s}}$ ($\hat{s} < s$):

$$d\sigma_f(s) = \int d\hat{s}\, H(s,\hat{s})\, d\hat{\sigma}_f(\hat{s}), \qquad 3.4.$$

where $d\hat{\sigma}_f (f \neq e)$ may be evaluated as

$$d\hat{\sigma}_f(\hat{s}) = \frac{1}{2\hat{s}} \left\{ \frac{1-P_e}{4} \sum_\beta \left|T^{ef}_{L\beta}\right|^2 + \frac{1+P_e}{4} \sum_\beta \left|T^{ef}_{R\beta}\right|^2 \right\} \frac{\hat{\beta}_f\, d\cos\hat{\theta}}{16\pi} \qquad 3.5.$$

for the e^- beam polarization $P_e = \pm|P|$, and the hatted variables are measured in the $f\bar{f}$ c.m. frame. The corresponding formula for small-angle Bhabha scattering, $e^+e^- \to e^+e^-$, is more complicated due to the presence of the smaller momentum-transfer scale $|t|$ and the importance of radiation from the final e^+e^- pairs, while the dominance of the t-channel exchange amplitudes allows calculation of the cross section independent of short-distance electroweak

physics. The small-angle Bhabha scattering process has therefore been used to monitor the luminosity, and all the other processes have been used to extract information on the electroweak physics at short distances. For these purposes, the radiator function $H(s, \hat{s})$ and the small-angle Bhabha scattering cross sections have been evaluated very accurately (29, 34) to better than 0.1%.

Because the experiments can observe only the convolution (Equation 3.4) of the short-distance cross section, it is necessary to make certain assumptions on the energy dependence of the short-distance electroweak amplitudes in order to measure the Z-boson properties. Near the Z-boson pole, the reduced amplitudes (Equation 3.3) (for $i = e_\alpha$ and $j = f_\beta$) can be approximately expressed as

$$M^{e\,f}_{\alpha\,\beta} \approx \frac{A + iB}{s} + \frac{M^e_\alpha(m_Z^2)\, M^f_\beta(m_Z^2) + (C + iD)(\sqrt{s} - m_Z)}{s - m_Z^2 + is(\Gamma_Z/m_Z)\theta(s)}, \qquad 3.6.$$

where A, B, C, and D are real constants that depend on the flavor f and chiralities α and β. The standard LEP analysis assumes standard-model predictions for those "background" contributions and determines from the data m_Z, Γ_Z, and various pseudo-observables at the Z pole that are obtained from the $Z \to f_\alpha \overline{f_\alpha}$ amplitudes,

$$\begin{aligned} M^f_\alpha(m_Z^2) = {} & (I_{3f\alpha} - Q_f \hat{s}^2)\left[\bar{g}_Z(m_Z^2) + \hat{g}_Z\, \mathrm{Re}\Gamma_1^{f\alpha}(m_Z^2)\right] \\ & + \hat{g}_Z \mathrm{Re}\left[I_{3f\alpha}\, \hat{c}^2\, \bar{\Gamma}_2^{f\alpha}(m_Z^2) + \Gamma_3^{f\alpha}(m_Z^2)\right. \\ & \left. - Q_f\left(\bar{s}^2(m_Z^2) - \hat{s}^2\right)\right]. \end{aligned} \qquad 3.7.$$

In the more sophisticated S-matrix analysis (33), the complex pole positions and residues are determined more model-independently. The following analysis adopts the standard data set that assumes the standard-model backgrounds, since possible effects of nonstandard physics on the measurements of (pseudo-)observables at the Z pole are expected to be very small.

Because all the pseudo-observables measured at the Z-pole experiments are expressed in terms of the real scalar amplitude M^f_α (Equation 3.7), it is useful to present their theoretical predictions. With the notation

$$g^f_\alpha \equiv \frac{M^f_\alpha(m_Z^2)}{\sqrt{4\sqrt{2}G_F m_Z^2}} \approx \frac{M^f_\alpha(m_Z^2)}{0.74070}, \qquad 3.8.$$

all the amplitudes can be expressed as follows:

$$g_L^\nu = 0.50214 + 0.453\,\Delta\bar{g}_Z^2, \tag{3.9a.}$$

$$g_L^e = -0.26941 - 0.244\,\Delta\bar{g}_Z^2 + 1.001\,\Delta\bar{s}^2, \tag{3.9b.}$$

$$g_R^e = 0.23201 + 0.208\,\Delta\bar{g}_Z^2 + 1.001\,\Delta\bar{s}^2, \tag{3.9c.}$$

$$g_L^u = 0.34694 + 0.314\,\Delta\bar{g}_Z^2 - 0.668\,\Delta\bar{s}^2, \tag{3.9d.}$$

$$g_R^u = -0.15466 - 0.139\,\Delta\bar{g}_Z^2 - 0.668\,\Delta\bar{s}^2, \tag{3.9e.}$$

$$g_L^d = -0.42451 - 0.383\,\Delta\bar{g}_Z^2 + 0.334\,\Delta\bar{s}^2, \tag{3.9f.}$$

$$g_R^d = 0.07732 + 0.069\,\Delta\bar{g}_Z^2 + 0.334\,\Delta\bar{s}^2, \tag{3.9g.}$$

$$g_L^b = -0.42109 - 0.383\,\Delta\bar{g}_Z^2 + 0.334\,\Delta\bar{s}^2 + \Delta g_L^b. \tag{3.9h.}$$

The m_t dependence of the Zb_Lb_L vertex correction in the amplitude g_L^b is parameterized by x_t (Equation 2.33) as (17)

$$\Delta g_L^b = 0.00044x_t + 0.00001x_t^2 + \left[g_L^b\right]_{\text{new}}, \tag{3.10.}$$

where possible new-physics contributions to the vertex function can be included. In the above parameterization, new-physics contributions through the gauge-boson propagator corrections are included in the terms $\Delta\bar{g}_Z^2$ and $\Delta\bar{s}^2$ through S_{new}, T_{new}, and U_{new} in Equations 2.31, and contributions to the vertex functions can be added to each amplitude as $[g_\alpha^f]_{\text{new}}$.

In terms of the above effective Z-decay amplitudes, the partial widths can be calculated as

$$\Gamma_f = \frac{G_F m_Z^3}{6\sqrt{2}\pi}\left[\left(g_V^f\right)^2 C_{fV} + \left(g_A^f\right)^2 C_{fA}\right]\left(1 + \frac{3}{4}Q_f^2\frac{\bar{\alpha}\left(m_Z^2\right)}{\pi}\right) \tag{3.11.}$$

where

$$g_V^f = g_L^f + g_R^f, \quad g_A^f = g_L^f - g_R^f, \tag{3.12.}$$

and the factors C_{fV} and C_{fA} contain both the finite f-mass effect and the QCD corrections for quarks. Their numerical values are listed in Table 1. In order to parameterize the α_s dependences of the QCD corrections, we introduce the parameter

$$x_s = \frac{\alpha_s(m_Z)_{\overline{\text{MS}}} - 0.118}{0.003}, \tag{3.13.}$$

in analogy to the parameters in Equation 2.33. The last term proportional to $\bar{\alpha}(m_Z^2)$ in Equation 3.11 accounts for the final-state QED correction.

Table 1 Numerical values of the factors C_{fV}, C_{fA} in Equation 3.11 for the Z partial widths; $x_s = (\alpha_s(m_Z) - 0.118)/0.003$

	C_{fV}	C_{fA}
u	$3.1166 + 0.0030x_s$	$3.1351 + 0.0040x_s$
$d = s$	$3.1166 + 0.0030x_s$	$3.0981 + 0.0021x_s$
c	$3.1167 + 0.0030x_s$	$3.1343 + 0.0041x_s$
b	$3.1185 + 0.0030x_s$	$3.0776 + 0.0030x_s$
ν	1	1
$e = \mu$	1	1
τ	1	0.9977

In terms of the partial widths, the hadronic and total widths of the Z boson are evaluated accurately as

$$\Gamma_h = \Gamma_u + \Gamma_c + \Gamma_d + \Gamma_s + \Gamma_b, \qquad 3.14a.$$

$$\Gamma_Z = 3\Gamma_\nu + \Gamma_e + \Gamma_\mu + \Gamma_\tau + \Gamma_h, \qquad 3.14b.$$

where three massless neutrinos are assumed to contribute to the invisible decay width Γ_{inv}. The LEP experiments measured m_Z, Γ_Z, the hadronic cross section at the Z pole,

$$\sigma_h^0 = \frac{12\pi}{m_Z^2}\frac{\Gamma_e\Gamma_h}{\Gamma_Z^2}, \qquad 3.15.$$

and various ratios of the partial widths,

$$R_l = \frac{\Gamma_h}{\Gamma_l}(l = e, \mu, \tau), \quad R_b = \frac{\Gamma_b}{\Gamma_h}, \quad R_c = \frac{\Gamma_c}{\Gamma_h}, \qquad 3.16.$$

since their measurement errors are least correlated. When the lepton universality is assumed, the ratio R_ℓ is measured under the constraint $R_\ell = R_e = R_\mu = 0.9977R_\tau$. It is worth noting here that from the three most accurately measured Z line-shape observables, Γ_Z, σ_h^0, and R_ℓ, one can directly determine the three partial widths Γ_h, Γ_e, and Γ_{inv} from the identity

$$\Gamma_Z = \Gamma_h + 2.9977\Gamma_e + \Gamma_{\text{inv}}. \qquad 3.17.$$

The effective number of the massless neutrinos, N_ν, is then determined via

$$\Gamma_{\text{inv}} = N_\nu\,[\Gamma_\nu]_{\text{SM}}. \qquad 3.18.$$

All the asymmetry parameters measured at LEP1 and SLC are expressed in terms of the left-right asymmetry parameters

$$A^f = \frac{\left(g_L^f\right)^2 - \left(g_R^f\right)^2}{\left(g_L^f\right)^2 + \left(g_R^f\right)^2} = \frac{2g_V^f g_A^f}{\left(g_V^f\right)^2 + \left(g_A^f\right)^2}. \qquad 3.19.$$

At LEP1 the τ lepton polarization measures $P_\tau = -A^\tau$, and the forward-backward (FB) asymmetry of the τ polarization measures the Z polarization along the e^- beam direction, A^e. At SLC the e^- beam-polarization asymmetry of the Z-production cross section measures $A^0_{LR} = A^e$, and the jet FB asymmetry of the beam-polarization asymmetry measures A^b and A^c. Polarization-averaged FB asymmetries measure the products

$$A^{0,f}_{FB} = \frac{3}{4} A^e A^f. \qquad 3.20.$$

Finally, from the FB asymmetry of the jet-charge parameters, one can extract the effective mixing angle

$$\sin^2 \theta^{\text{lept}}_{\text{eff}} \equiv \frac{g^e_R}{2\left(g^e_R - g^e_L\right)} = \frac{1}{4}\left(1 - \frac{g^e_V}{g^e_A}\right) \qquad 3.21.$$

by assuming that there is no significant new-physics contribution to the flavor dependences of the amplitudes in Equation 3.9. In the following analysis, the jet-charge asymmetry data is dropped when this assumption does not hold (e.g. in the analysis of Z–Z' mixing). The reported asymmetry parameters have been corrected for the final fermion mass effect as well as for QED and QCD radiation effects. The lepton universality thus implies $A^\ell = A^e = A^\mu = A^\tau$. LEP experiments (35) have provided a detailed report of perturbative as well as nonperturbative QCD corrections to the jet asymmetries.

The standard-model predictions for all the above observables are easily calculated using the parameterizations of Equations 3.9, 2.30, 2.32, and 3.10. New-physics predictions can also be evaluated by accounting for S_{new}, T_{new}, U_{new} in Equation 2.31, possible new contributions to Equations 2.26 and 2.28, and possible additional terms $[g^f_\alpha]_{\text{new}}$ in Equation 3.9.

Within the standard model, or in models where the major new-physics contribution enters through the gauge-boson propagator corrections and the Zb_Lb_L vertex correction only, we find the following parameterizations. The three accurately measured partial widths are

$$\Gamma_\nu[\text{GeV}] = 0.16730 + 0.302\,\Delta\bar{g}^2_Z, \qquad 3.22a.$$

$$\Gamma_e[\text{GeV}] = 0.08403 + 0.152\,\Delta\bar{g}^2_Z - 0.050\,\Delta\bar{s}^2, \qquad 3.22b.$$

$$\Gamma_h[\text{GeV}] = 1.7434 + 3.15\,\Delta\bar{g}^2_Z - 2.50\,\Delta\bar{s}^2 + 0.0017\,x'_s, \qquad 3.22c.$$

where the parameter

$$x'_s \equiv \frac{\alpha'_s - 0.118}{0.003} = x_s - 1044\,\Delta g^b_L \qquad 3.23.$$

appears, reflecting the fact that only the combination (17, 28)

$$\alpha_s' \equiv \alpha_s(m_Z)_{\overline{\rm MS}} + 3.186\,\frac{\delta\Gamma_h}{\Gamma_h^{(0)}} \qquad 3.24.$$

is measured accurately from the Z parameters. Here $\Gamma_h^{(0)}$ denotes the reference standard-model prediction and $\delta\Gamma_h = \Gamma_h - \Gamma_h^{(0)}$, both evaluated at $\alpha_s = 0.118$. If only the partial width Γ_b deviates from the reference standard-model prediction, then

$$\frac{\delta\Gamma_h}{\Gamma_h^{(0)}} = \frac{\delta R_b}{1-R_b} = -0.983\,\Delta g_L^b + 0.175\,\left[g_R^b\right]_{\rm new} \qquad 3.25.$$

holds. By setting $[g_R^b]_{\rm new} = 0$, we obtain the combination of Equation 3.23. The predictions are as follows:

$$\Gamma_Z\,[\text{GeV}] = 2.4972 + 4.51\,\Delta\bar{g}_Z^2 - 2.65\,\Delta\bar{s}^2 + 0.0017 x_s', \qquad 3.26a.$$

$$\sigma_h^0[\text{nb}] = 41.474 + 0.01\,\Delta\bar{g}_Z^2 + 3.92\,\Delta\bar{s}^2 - 0.016\,x_s', \qquad 3.26b.$$

$$R_\ell = 20.747 + 0.05\,\Delta\bar{g}_Z^2 - 17.4\,\Delta\bar{s}^2 + 0.020\,x_s', \qquad 3.26c.$$

$$R_b = 0.2157 + 0.002\,\Delta\bar{g}_Z^2 + 0.04\,\Delta\bar{s}^2 - 0.78\,\Delta g_L^b, \qquad 3.26d.$$

$$R_c = 0.1721 + 0.000\,\Delta\bar{g}_Z^2 - 0.06\,\Delta\bar{s}^2 + 0.18\,\Delta g_L^b, \qquad 3.26e.$$

$$A_{FB}^{0,\ell} = 0.0165 + 0.002\,\Delta\bar{g}_Z^2 - 1.75\,\Delta\bar{s}^2, \qquad 3.26f.$$

$$A_{FB}^{0,b} = 0.1040 + 0.005\,\Delta\bar{g}_Z^2 - 5.58\,\Delta\bar{s}^2 - 0.03\,\Delta g_L^b, \qquad 3.26g.$$

$$A_{FB}^{0,c} = 0.0744 + 0.004\,\Delta\bar{g}_Z^2 - 4.32\,\Delta\bar{s}^2, \qquad 3.26h.$$

$$A^\ell = 0.1484 + 0.007\,\Delta\bar{g}_Z^2 - 7.86\,\Delta\bar{s}^2, \qquad 3.26i.$$

$$A_b = 0.935 + 0.001\,\Delta\bar{g}_Z^2 - 0.65\,\Delta\bar{s}^2 - 0.30\,\Delta g_L^b, \qquad 3.26j.$$

$$A_c = 0.668 + 0.003\,\Delta\bar{g}_Z^2 - 3.45\,\Delta\bar{s}^2, \qquad 3.26k.$$

$$\sin^2\theta_{\rm eff}^{\rm lept} = 0.23135 - 0.001\,\Delta\bar{g}_Z^2 + 0.9982\,\Delta\bar{s}^2. \qquad 3.26l.$$

By comparing the coefficients of each term in Equation 3.26 with the corresponding experimental errors in Table 2, we find that the parameter $\Delta\bar{g}_Z^2$ is constrained essentially by Γ_Z; x_s' is constrained by R_ℓ and Γ_Z; $\Delta\bar{s}^2$ is constrained by A_{LR}^0, $A_{FB}^{0,b}$, $A_{FB}^{0,\ell}$, A^τ, and A^e, in decreasing order of significance; and the parameter Δg_L^b is constrained essentially by R_b. By comparing Equation 3.26l with Equation 2.29b, we confirm an accurate relation (17) $\sin\theta_{\rm eff}^{\rm lept} = \bar{s}^2(m_Z^2) + 0.0010$.

If both g_L^b and g_R^b are allowed to have significant new-physics contributions, then we have

Table 2 Electroweak measurements at LEP, SLC, and the Tevatron[a]

	data	SM	pull
LEP 1			
line-shape & FB asym.:			
m_Z (GeV)	91.1867 ± 0.0020	—	—
Γ_Z (GeV)	2.4948 ± 0.0025	2.4972	−1.0
σ_h^0 (nb)	41.486 ± 0.053	41.474	0.2
R_ℓ	20.775 ± 0.027	20.747	1.1
$A_{\rm FB}^{0,\ell}$	0.0171 ± 0.0010	0.0165	0.6
for each lepton:			
R_e	20.757 ± 0.056	20.747	0.2
R_μ	20.783 ± 0.037	20.747	1.0
R_τ	20.823 ± 0.050	20.795	0.6
$A_{\rm FB}^{0,e}$	0.0160 ± 0.0024	0.0165	−0.2
$A_{\rm FB}^{0,\mu}$	0.0163 ± 0.0014	0.0165	−0.1
$A_{\rm FB}^{0,\tau}$	0.0192 ± 0.0018	0.0165	1.5
τ polarization:			
A_τ	0.1411 ± 0.0064	0.1484	−1.1
A_e	0.1399 ± 0.0073	0.1484	−1.2
b and c quark results:			
R_b	0.2170 ± 0.0009	0.2157	1.4
R_c	0.1734 ± 0.0048	0.1721	0.3
$A_{FB}^{0,b}$	0.0984 ± 0.0024	0.1040	−2.3
$A_{FB}^{0,c}$	0.0741 ± 0.0048	0.0744	−0.1
jet charge asymmetry:			
$\sin^2\theta_{\rm eff}^{\rm lept}$	0.2322 ± 0.0010	0.2314	0.8
SLC			
A_{LR}^0	0.1547 ± 0.0032	0.1484	2.0
A_b	0.900 ± 0.050	0.935	−0.7
A_c	0.650 ± 0.058	0.668	−0.3
Tevatron + LEP 2			
m_W (GeV)	80.43 ± 0.084	80.402	0.4

[a]The reference standard-model predictions and the corresponding "pulls" are given for $m_t = 175$ GeV, $m_H = 100$ GeV, $\alpha_s(m_Z) = 0.118$ and $1/\bar{\alpha}(m_Z^2) = 128.75$ (see Equation 2.19). Correlation matrix elements of the Z line-shape parameters and those for the heavy-quark parameters are found in (33). The data of R_ℓ and $A_{\rm FB}^{0,\ell}$ are obtained by assuming e-μ-τ universality.

$$R_b = [R_b]_{\rm SM} - 0.78\left[g_L^b\right]_{\rm new} + 0.14\left[g_R^b\right]_{\rm new}, \quad 3.27a.$$

$$R_c = [R_c]_{\rm SM} + 0.18\left[g_L^b\right]_{\rm new} - 0.03\left[g_R^b\right]_{\rm new}, \quad 3.27b.$$

$$A_{\rm FB}^{0,b} = \left[A_{\rm FB}^{0,b}\right]_{\rm SM} - 0.03\left[g_L^b\right]_{\rm new} - 0.18\left[g_R^b\right]_{\rm new}, \quad 3.27c.$$

$$A_b = [A_b]_{\rm SM} - 0.30\left[g_L^b\right]_{\rm new} - 1.63\left[g_R^b\right]_{\rm new}, \quad 3.27d.$$

and x_s' of Equation 3.23 should now read $x_s' = x_s - 1044\,\Delta g_L^b + 180\,[g_R^b]_{\rm new}$ via the identity (3.25).

3.2 *Direct Measurements of m_W, m_t, m_H, and α_s*

The W-boson mass has been measured at Fermilab's Tevatron $p\bar{p}$ collider. The average of CDF and DØ measurements gives (36)

$$m_W[\text{GeV}] = 80.41 \pm 0.09. \quad 3.28.$$

More recently, the LEP2 experiments at CERN determined m_W from the $e^+e^- \to W^+W^-$ cross section at threshold and from the invariant mass of the decaying W at high energies. By combining the results of the four experiments and the two methods, one finds (33)

$$m_W[\text{GeV}] = 80.48 \pm 0.14. \quad 3.29.$$

The following analysis uses the world average of the above two measurements,

$$m_W[\text{GeV}] = 80.43 \pm 0.084. \quad 3.30.$$

In the standard model and in many of its extensions, the top-quark mass and the Higgs-boson mass are essential in determining the magnitudes of the quantum corrections. The CDF and DØ experiments at the Tevatron find (37)

$$m_t[\text{ GeV}] = 175.6 \pm 5.5 \quad 3.31.$$

from the analysis of the sequential decays of the pair-produced top quarks. As for the Higgs boson, the negative results of search experiments at LEP lead to the lower mass bound (38)

$$m_H[\text{ GeV}] > 77 \quad (95\%\ \text{CL}), \quad 3.32.$$

in the minimal standard model. The bound is weaker in models with more than one Higgs boson.

Finally, the strong-coupling constant α_s determines the magnitudes of the Z-boson hadronic width Γ_h at the one-loop level and also determines the magnitudes of all the radiative effects with virtual quarks at two- and higher-loop orders. In the following analysis, we adopt the world average (9)

$$\alpha_s(m_Z)_{\overline{\rm MS}} = 0.118 \pm 0.003 \quad 3.33.$$

as our standard reference. Many of the results will be shown in such a way that consequences of the future improved measurements of m_W, m_t, m_H, α_s, and δ_α can be readily studied.

Table 2 lists all the electroweak data (33) on the weak-boson properties measured at LEP, SLC, and the Tevatron. Correlations among some of the errors are non-negligible (33). The table also shows the standard-model predictions at our reference point, $m_t = 175$ GeV, $m_H = 100$ GeV, $\alpha_s(m_Z) = 0.118$, and $1/\bar{\alpha}(m_Z^2) = 128.75$, and the corresponding "pull" representing the deviation of the measured mean value from the reference prediction in units of the 1-σ error. The total χ^2 of the standard model at the reference point is 20.3 for 19 data points. As shown below, our reference point is close to the point at which the standard model gives the best description of the data.

3.3 *Observables at Low Energies*

This subsection lists the data and theoretical predictions for the electroweak observables in low-energy neutral-current experiments. Thanks to the precision determination of the Z-boson properties at the Z factories, the low-energy data shed new light on our search for new physics. The experimental results on the parity-odd asymmetries in the l–q sector (Sections 3.3.1–3.3.5) are parameterized in terms of model-independent parameters C_{1q} and C_{2q} (39), and results on μ charge-polarization asymmetry (Section 3.3.2) are given in terms of the parameters C_{3q} (41). The ν_μ scattering data (Sections 3.3.6–3.3.7) are expressed in terms of the parameters $(g_{L\,\alpha}^{\nu_\mu f})$. All the model-independent parameters can be expressed compactly (17) in terms of the reduced helicity amplitudes of Equation 3.3,

$$C_{1q} = \frac{1}{2\sqrt{2}\,G_F}\left(M_{LL}^{\ell q} + M_{LR}^{\ell q} - M_{RL}^{\ell q} - M_{RR}^{\ell q}\right), \qquad 3.34a.$$

$$C_{2q} = \frac{1}{2\sqrt{2}\,G_F}\left(M_{LL}^{\ell q} - M_{LR}^{\ell q} + M_{RL}^{\ell q} - M_{RR}^{\ell q}\right), \qquad 3.34b.$$

$$C_{3q} = \frac{1}{2\sqrt{2}\,G_F}\left(-M_{LL}^{\ell q} + M_{LR}^{\ell q} + M_{RL}^{\ell q} - M_{RR}^{\ell q}\right), \qquad 3.34c.$$

$$g_{L\,\alpha}^{\nu_\mu f} = \frac{1}{2\sqrt{2}\,G_F}\left(-M_{L\,\alpha}^{\nu_\mu f}\right), \qquad 3.34d.$$

and accurate theoretical predictions are reached by evaluating the amplitudes at the relevant momentum-transfer scale. These model-independent parameters allow us to study the implications of the low-energy neutral-current experiments in a wide class of models (see 40, 41 for a comprehensive review).

3.3.1 SLAC *ed* EXPERIMENT The parity asymmetry in the inelastic scattering of polarized electrons off a deuterium target was measured at SLAC (42). The

Table 3 Electroweak measurements in the low-energy neutral-current experiments[a]

	data	SM	pull
$\ell-q$ scattering:			
SLAC			
$A_{\rm SLAC}$	0.80 ± 0.058	0.745	0.9
CERN			
$A_{\rm CERN}$	-1.57 ± 0.38	-1.42	-0.4
Bates			
$C_{1u} + C_{1d}$	-0.137 ± 0.033	-0.152	0.5
Mainz			
$A_{\rm Mainz}$	-0.94 ± 0.19	-0.876	-0.3
Atomic Parity Violation:			
Q_W ($^{133}_{55}$Cs)	-72.08 ± 0.92	-73.07	1.1
Q_W ($^{205}_{81}$Tl)	-115.0 ± 4.2	-116.6	0.4
ν_μ-quark scattering:			
CDHS and others			
g_L^2	0.2980 ± 0.0044	0.3027	-1.1
g_R^2	0.0307 ± 0.0047	0.0298	0.2
δ_L^2	-0.0589 ± 0.0237	-0.0641	0.2
δ_R^2	0.0206 ± 0.0160	0.0179	0.2
CCFR			
$K_{\rm CCFR}$	0.5820 ± 0.0049	0.5786	0.7
ν_μ-e scattering:			
$g_{L\,L}^{\nu_\mu e}$	-0.269 ± 0.011	-0.273	0.4
$g_{L\,R}^{\nu_\mu e}$	0.234 ± 0.011	0.233	0.1

[a]The reference standard-model predictions and the corresponding "pulls" are given for $m_t = 175$ GeV, $m_H = 100$ GeV and $1/\bar{\alpha}(m_Z^2) = 128.75$ (see Equation 2.19). The error correlation matrix elements are found e.g. in Argento (43).

experiment constrains $2C_{1u} - C_{1d}$ and $2C_{2u} - C_{2d}$. The most stringent constraint shown in Table 3 is found for the combination

$$A_{\rm SLAC} = 2C_{1u} - C_{1d} + 0.206\,(2C_{2u} - C_{2d}) \qquad 3.35a.$$

$$= 0.745 - 0.016\,\Delta S + 0.016\,\Delta T, \qquad 3.35b.$$

where the theoretical prediction (17) is evaluated at $\langle Q^2 \rangle = 1.5$ GeV^2.

3.3.2 CERN $\mu^\pm$C EXPERIMENT The CERN $\mu^\pm$C experiment (43) measured the charge and polarization asymmetry of deep-inelastic muon scattering off a ^{12}C target. The experiment constrains $2C_{2u} - C_{2d}$ and $2C_{3u} - C_{3d}$. The most stringent constraint shown in Table 3 is found for the combination

$$A_{\rm CERN} = 2C_{3u} - C_{3d} + 0.777\,(2C_{2u} - C_{2d}) \qquad 3.36a.$$

$$= -1.42 - 0.016\,\Delta S - 0.0007\,\Delta T, \qquad 3.36b.$$

where the theoretical prediction (41) is evaluated at $\langle Q^2\rangle = 50$ GeV^2.

3.3.3 BATES eC EXPERIMENT The polarization asymmetry of electron elastic scattering off a ^{12}C target was measured at Bates (44). The experiment (see Table 3) constrains the combination

$$C_{1u} + C_{1d} = -0.1522 - 0.0023\,\Delta S + 0.0004\,\Delta T, \qquad 3.37.$$

where the theoretical prediction (41) is evaluated at $\langle Q^2\rangle = 0.0225$ GeV^2.

3.3.4 MAINZ eBe EXPERIMENT The polarization asymmetry of electron quasi-elastic scattering off a ^{9}Be target was measured at Mainz (45). The data shown in Table 3 are for the combination

$$A_{\rm Mainz} = -2.73C_{1u} + 0.65C_{1d} - 2.19C_{2u} + 2.03C_{2d} \qquad 3.38.$$

$$= -0.875 + 0.043\,\Delta S - 0.035\,\Delta T, \qquad 3.39.$$

where the theoretical prediction (41) is evaluated at $\langle Q^2\rangle = 0.2025$ GeV^2.

3.3.5 ATOMIC PARITY VIOLATION The experimental results of parity violation in the atom are often given in terms of the weak charge $Q_W(A, Z)$ of nuclei (46), which can be expressed as

$$Q_W(A, Z) = 2ZC_{1p} + 2(A - Z)C_{1n}, \qquad 3.40.$$

where the coefficients C_{1p} and C_{1n} are estimated as (17, 47)

$$C_{1p} = 2C_{1u} + C_{1d} + 0.0028, \qquad 3.41a.$$

$$C_{1n} = C_{1u} + 2C_{1d} + 0.0028, \qquad 3.41b.$$

including long-distance photonic corrections (47). By evaluating the reduced amplitudes at zero momentum transfer, we find

$$C_{1p} = 0.0360 - 0.0068\,\Delta S + 0.0048\,\Delta T, \qquad 3.42a.$$

$$C_{1n} = -0.4938 - 0.0037\,\Delta T. \qquad 3.42b.$$

Table 3 displays the data for $^{133}_{55}$Cs (48, 49) and $^{205}_{81}$Tl (50, 51). The standard-model predictions are (41)

$$Q_W^{\rm SM}\left(^{133}_{55}{\rm Cs}\right) = -73.07 - 0.75\,\Delta S - 0.05\,\Delta T, \qquad 3.43a.$$

$$Q_W^{\rm SM}\left(^{205}_{81}{\rm Tl}\right) = -116.6 - 1.10\,\Delta S - 0.13\,\Delta T. \qquad 3.43b.$$

Because of the cancellation between the proton and neutron contributions, the weak charges depend weakly on ΔT, while their dependences on ΔS are enhanced (24, 40, 52) by the number of protons.

3.3.6 NEUTRINO-QUARK SCATTERING For ν_μ-quark scattering, the experimental results up to 1988 were summarized (53) in terms of the model-independent parameters g_L^2, g_R^2, δ_L^2, δ_R^2. More recently, the CCFR experiment at the Tevatron measured the combination (54)

$$K_{\rm CCFR} = 1.7897 g_L^2 + 1.1479 g_R^2 - 0.0916 \delta_L^2 - 0.0782 \delta_R^2. \qquad 3.44.$$

Table 3 includes these data. The standard-model predictions are calculated from our reduced amplitudes (Equation 3.34d) as follows (17, 41):

$$g_\alpha^2 = \left(g_{L\alpha}^{\nu_\mu u}\right)^2 + \left(g_{L\alpha}^{\nu_\mu d}\right)^2, \quad \delta_\alpha^2 = \left(g_{L\alpha}^{\nu_\mu u}\right)^2 - \left(g_{L\alpha}^{\nu_\mu d}\right)^2, \qquad 3.45.$$

for $\alpha = L$ and R, respectively, where

$$g_{L\,L}^{\nu_\mu u} = 0.3449 - 0.0023\,\Delta S + 0.0041\,\Delta T, \qquad 3.46a.$$

$$g_{L\,R}^{\nu_\mu u} = -0.1540 - 0.0023\,\Delta S + 0.0004\,\Delta T, \qquad 3.46b.$$

$$g_{L\,L}^{\nu_\mu d} = -0.4276 + 0.0012\,\Delta S - 0.0039\,\Delta T, \qquad 3.46c.$$

$$g_{L\,R}^{\nu_\mu d} = 0.0771 + 0.0012\,\Delta S - 0.0002\,\Delta T. \qquad 3.46d.$$

The above predictions are obtained at the momentum transfer of $\langle Q^2 \rangle = 35\ {\rm GeV}^2$ relevant for the CCFR experiments (54). The estimates are also valid (41) for the data of Fogli & Haidt (53), in which a typical scale is $\langle Q^2 \rangle = 20\ {\rm GeV}^2$.

It is worth noting that the standard-model predictions for the parameter K depend almost solely on m_W. In fact, from Equation 3.46 we find

$$K_{\rm CCFR} = 0.5786 - 0.0036\,\Delta S + 0.0108\,\Delta T \qquad 3.47a.$$

$$= 0.5786 + 0.00143(x_t - 0.83 x_H - 0.19 x_H^2 - 0.02 x_t x_H), \qquad 3.47b.$$

whereas from Equation 2.30c we find (at $x_\alpha = 0$)

$$m_W = 80.402 - 0.288\,\Delta S + 0.418\,\Delta T + 0.337\,\Delta U \qquad 3.48a.$$

$$= 80.402 + 0.0638(x_t - 0.94 x_H - 0.14 x_H^2 - 0.02 x_t x_H), \qquad 3.48b.$$

in GeV units. We thus find the identity

$$K_{\rm CCFR} = 0.5786 + 0.022\,[m_W - 80.402] + 0.00016 x_H (1 - 0.41 x_H). \qquad 3.49.$$

The last term in the above equation is at most 0.0001 in the whole allowed m_t and m_H range. Nevertheless, as the above derivation makes clear, such identification holds only within the minimal standard model. If the data are to be useful in constraining new physics, they must be presented in terms of the model-independent parameters.

3.3.7 NEUTRINO-ELECTRON SCATTERING The $\nu_\mu e$ scattering experiments measure the neutral currents in a purely leptonic channel. Table 3 gives the combined results (41, 55). The theoretical predictions (41),

$$g_{L\,L}^{\nu_\mu e} = -0.273 + 0.0033\,\Delta S - 0.0042\,\Delta T, \qquad 3.50a.$$

$$g_{L\,R}^{\nu_\mu e} = 0.233 + 0.0033\,\Delta S - 0.0006\,\Delta T, \qquad 3.50b.$$

are evaluated at $\langle Q^2 \rangle = 2m_e E_\nu$ at $E_\nu = 25.7$ GeV for the CHARM II experiment (55).

4. INTERPRETATIONS OF THE ELECTROWEAK DATA

Subsection 4.1 examines the universality of the quark and lepton couplings to the Z boson, which is one of the most fundamental consequences of the gauge principle. In Subsection 4.2, we study constraints on the gauge-symmetry–breaking physics within the $\mathrm{SU(2)_L} \otimes \mathrm{U(1)_Y}$ models, and in Subsection 4.3 we study constraints on the parameters of the minimal standard model. The last subsection is a brief overview of implications of precision electroweak measurements for physics beyond the standard model.

4.1 *Universality of the Effective Z-Boson Couplings*

4.1.1 TEST OF LEPTON UNIVERSALITY Table 2 gives the partial width ratios $R_l = \Gamma_h/\Gamma_l$ and the FB asymmetries $A_{\mathrm{FB}}^{0,l}$ for e, μ, and τ separately. Along with the data on Γ_Z and σ_h^0, the R_l data determine the partial widths Γ_e, Γ_μ, and Γ_τ separately,

$$\Gamma_e[\mathrm{GeV}] = 0.08394 \pm 0.00014, \qquad 4.1a.$$

$$\Gamma_\mu[\mathrm{GeV}] = 0.08384 \pm 0.00020, \qquad 4.1b.$$

$$\Gamma_\tau[\mathrm{GeV}] = 0.08368 \pm 0.00024, \qquad 4.1c.$$

and the hadronic and the invisible widths

$$\Gamma_h[\mathrm{GeV}] = 1.7432 \pm 0.0023, \qquad 4.2a.$$

$$\Gamma_{\mathrm{inv}}[\mathrm{GeV}] = 0.5001 \pm 0.0018. \qquad 4.2b.$$

From Equation 3.11, the leptonic widths constrain the squared sum $(g_V^l)^2 + (g_A^l)^2$, while the Z-pole asymmetries constrain the ratio $(g_V^l)/(g_A^l)$ via the parameters A_f (3.19). All six effective couplings can hence be constrained directly by the Z-pole data (see Table 4). Here we show the constraints on deviations from their reference standard-model values in Equation 3.9: $g_V^l = -0.00374 + \Delta g_V^l$ and $g_A^l = -0.50142 + \Delta g_A^l$.

Table 4 Summary of constraints on $(\Delta g_A^l, \Delta g_V^l)$ for $l = e, \mu, \tau$ from Z-pole measurements[a]

	Δg_A^f	Δg_V^f	$\rho_{\rm corr}$
e (LEP)	0.00022 ± 0.00043	0.00067 ± 0.00145	-0.23
μ (LEP)	0.00057 ± 0.00065	-0.00002 ± 0.00355	-0.39
τ (LEP)	0.00043 ± 0.00073	0.00072 ± 0.00152	-0.12
ℓ (LEP)	0.00035 ± 0.00032	0.00059 ± 0.00085	-0.17
e (LEP+SLC)	0.00035 ± 0.00042	-0.00105 ± 0.00071	-0.08
ℓ (LEP+SLC)	0.00043 ± 0.00031	-0.00054 ± 0.00058	-0.10

[a]First four lines: results obtained using LEP data alone; last two lines: combined results of LEP/SLC data.

All determinations of the effective couplings are consistent with each other and with the reference standard-model predictions. The largest deviation is between the g_V^e value from LEP and that from SLC but it is not significant ($\sim$1-σ). The assumption that universal parameters g_V^ℓ and g_A^ℓ describe nine leptonic observables, the three leptonic widths of Equation 4.1 and the six asymmetries in Table 2, gives $\chi^2_{\rm min}/({\rm d.o.f}) = 8.2/7$ [32% confidence level (CL)].

It is also worth noting that the invisible-width data (Equation 4.2b) constrain the effective number of neutrinos via Equation 3.18, $N_\nu = 2.989 - 5.40\,\Delta\bar{g}_Z^2 \pm 0.011$, where the parameterization (3.22a) is used. Systematic uncertainty can be minimized by using the ratio $\Gamma_{\rm inv}/\Gamma_\ell$ (33), and

$$N_\nu = 2.993 \pm 0.011 \qquad 4.3.$$

is obtained in the standard model. That this number agrees precisely with 3 can be regarded as evidence that all three neutrinos couple universally to the Z boson.

4.1.2 CONSTRAINTS ON b, τ-SECTOR One of the fundamental problems of particle physics is the replication of quarks and leptons and the origin of their masses. According to many theoretical ideas in flavor physics, the third-generation quarks and leptons behave differently from those of the first two generations. In some models, new flavor-dependent interactions directly affect the Z couplings through mixing between the standard-model Z boson and a new vector boson that couples to b and τ, or mixing between b, τ and new fermions. More generally, flavor-dependent new interactions are expected to affect the Z couplings to the third-generation quarks and leptons through radiative corrections. We can study the consequences of such deviations from flavor universality by introducing new-physics contributions to the effective vertices

g_α^f in Equation 3.9,

$$g_\alpha^f = \left[g_\alpha^f\right]_{\rm SM} + \left[g_\alpha^f\right]_{\rm new}, \tag{4.4.}$$

for $f = b, \tau, \nu_\tau$, and $\alpha = L, R$.

The constraint on the ν_τ vertex can be inferred directly from Equation 4.3,

$$\left[g_L^{\nu_\tau}\right]_{\rm new} = -0.0018 \pm 0.0028, \tag{4.5.}$$

and those for the $Z\tau\tau$ vertices are found to be

$$\left.\begin{aligned}\left[g_V^\tau\right]_{\rm new} &= 0.0006 \pm 0.0016\\ \left[g_A^\tau\right]_{\rm new} &= 0.0003 \pm 0.0006\end{aligned}\right\} \quad \rho_{\rm corr} = -0.16. \tag{4.6.}$$

All three vertices are consistent with the standard model, and new-physics contributions to them are constrained severely, especially for g_A^τ.

On the other hand, for the Zbb vertices we find

$$\left[g_R^b\right]_{\rm new} = 0.0257 \pm 0.0094, \tag{4.7a.}$$

$$\left[g_L^b\right]_{\rm new} = -0.0019 + 0.239\left[g_R^b\right]_{\rm new} \pm 0.0009. \tag{4.7b.}$$

The results can be understood by examining the expressions of Equation 3.27 and Table 2. The two deviations found in Table 2, those of R_b and $A_{\rm FB}^{0,b}$, can be absorbed into the two new parameters $[g_L^b]_{\rm new}$ and $[g_R^b]_{\rm new}$. The above results simply summarize the present status of electroweak measurements on the Zbb couplings. One should note, however, that the magnitude of $[g_R^b]_{\rm new}$ required to improve the fit is as large as 30% of its standard-model value, Equation 3.9g, and at the same time $[g_L^b]_{\rm new}$ should satisfy the stringent constraint of Equation 4.7b. Below, we set $[g_R^b]_{\rm new} = 0$ but retain Δg_L^b as a free parameter, since possible deviation from the standard model at the 0.5% level can be accounted for in various models.

4.2 *Interpretation in the* $\mathrm{SU(2)_L \otimes U(1)_Y}$ *Models*

In generic $\mathrm{SU(2)_L \otimes U(1)_Y}$ models, where new-physics effects are significant only in the gauge-boson propagator corrections and possibly in the Zb_Lb_L vertex correction, all the Z-pole observables are parameterized by the two effective coupling factors, $\Delta\bar{g}_Z^2$ and $\Delta\bar{s}^2$, and Δg_L^b (see Equation 3.26). The α_s dependence enters only through the combination x_s' (Equation 3.23). From the 14 Z-pole quantities of Table 2 we find

$$\left.\begin{aligned}\Delta\bar{g}_Z^2 &= -0.00044 - 0.00032\,x_s' \pm 0.00056\\ \Delta\bar{s}^2 &= 0.00012 + 0.00003\,x_s' \pm 0.00023\end{aligned}\right\} \quad \rho_{\rm corr} = 0.24, \tag{4.8a.}$$

$$\chi^2_{\rm min} = 13.8 + \left(\frac{\alpha_s' - 0.1216}{0.0036}\right)^2 + \left(\frac{\Delta g_L^b + 0.0017}{0.0011}\right)^2. \qquad 4.8b.$$

The above results summarize all the information that we obtain from the Z-pole measurements in this class of models. At the reference point $\alpha_s = 0.118$ and $\Delta g_L^b = 0$, the above two-parameter fit finds $\chi^2_{\rm min}/({\rm d.o.f}) = 17.2/(14-2)$ (14% CL).

If the new-physics contribution to the difference between $\bar{g}_Z^2(m_Z^2)$ and $\bar{g}_Z^2(0)$ (Equation 2.28) is small, then the above results can be expressed in terms of the S and T parameters:

$$\left.\begin{aligned} \Delta S &= -0.041 - 0.044\, x_s' + 0.064\, x_\alpha \pm 0.12 \\ \Delta T &= -0.109 - 0.078\, x_s' \pm 0.13 \end{aligned}\right\} \quad \rho_{\rm corr} = 0.86. \qquad 4.9.$$

The above parameterization is valid for $m_H > 70$ GeV, where the m_H dependence of the difference (Equation 2.28) is negligible. The low-energy data also constrain S and T. We find from the 13 measurements of Table 3

$$\left.\begin{aligned} \Delta S &= -1.13 + 0.12\, x_\alpha \pm 1.00 \\ \Delta T &= -0.50 \pm 0.50 \end{aligned}\right\} \quad \rho_{\rm corr} = 0.71, \qquad 4.10.$$

with $\chi^2_{\rm min}/{\rm d.o.f} = 3.7/(13-2)$. The two results, Equations 4.9 and 4.10, are consistent. Combining the Z-pole and low-energy data, we find

$$\left.\begin{aligned} \Delta S &= -0.056 - 0.038\, x_s' + 0.064\, x_\alpha \pm 0.12 \\ \Delta T &= -0.124 - 0.069\, x_s' \pm 0.13 \end{aligned}\right\} \quad \rho_{\rm corr} = 0.85, \qquad 4.11a.$$

$$\chi^2_{\rm min} = 18.6 + \left(\frac{\alpha_s' - 0.1216}{0.0036}\right)^2 + \left(\frac{\Delta g_L^b + 0.0017}{0.0011}\right)^2. \qquad 4.11b.$$

It is clear that the low-energy data has only minor (but not totally negligible) effects on constraining the S and T parameters.

The m_W measurement constrains the combination Δm_W of ΔS, ΔT, ΔU, and x_α (Equation 2.30c). The data (Equation 3.30) give

$$\Delta U - 0.855\, \Delta S + 1.240\, \Delta T = 0.083 - 0.036\, x_\alpha \pm 0.25. \qquad 4.12.$$

The above results, Equations 4.8, 4.10, and 4.12, or Equations 4.11 and 4.12, summarize all the electroweak measurements in generic models in which new physics affects only the gauge-boson propagator corrections and the Zb_Lb_L vertex function. From the above parameterizations of the fit, it is possible to extract constraints on the electroweak parameters ΔS, ΔT, and ΔU by

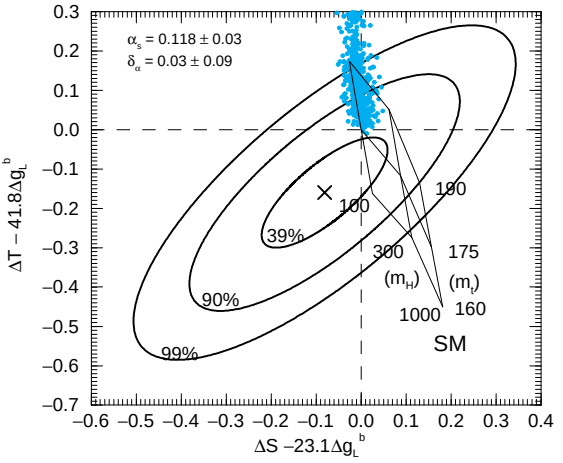

Figure 1 The ΔS and ΔT fit to all electroweak data. The three contours correspond to $\Delta\chi^2 = 1$, $\Delta\chi^2 = 4.61$, and $\Delta\chi^2 = 9.21$, respectively. The minimum of χ^2 is marked by $\times$. The dots represent possible contributions of supersymmetric particles (see Section 4.4.1).

using current knowledge of α_s and $\bar{\alpha}(m_Z^2)$. For instance, with the estimates of Equations 3.33 and 2.22a, we find

$$\left.\begin{aligned} \Delta S - 23.1\,\Delta g_L^b &= -0.081 \pm 0.14 \\ \Delta T - 41.8\,\Delta g_L^b &= -0.160 \pm 0.14 \end{aligned}\right\} \quad \rho_{\text{corr}} = 0.77, \qquad 4.13a.$$

$$\Delta U - 0.855\,\Delta S + 1.240\,\Delta T = 0.083 \pm 0.25, \qquad 4.13b.$$

$$\chi^2_{\text{min}} = 18.6 + \left(\frac{\Delta g_L^b + 0.0015}{0.0009}\right)^2. \qquad 4.13c.$$

Figure 1 shows the constraint of Equation 4.13a. The standard-model predictions are shown as functions of (m_t, m_H), since ΔS, ΔT, and Δg_L^b all depend on m_t and m_H in the standard model. Because the term Δg_L^b is constrained by the data as $\Delta g_L^b = -0.015 \pm 0.0009$ (Equation 4.13c), the data favor slightly negative values of ΔS and ΔT.

4.3 *Constraints on the Standard-Model Parameters*

It is apparent from Figure 1 that the data favor the region with $m_t \lesssim 175$ GeV and $m_H \lesssim$ a few hundred GeV in the standard model.

The m_W constraint (Equation 4.13b) also favors $m_H \lesssim$ a few hundred GeV for $m_t \sim 175$ GeV. In this subsection, we examine the constraints on the standard-model parameters from the electroweak measurements.

The standard-model predictions are uniquely determined when the four parameters m_t, m_H, δ_α, and α_s are given. Using all the electroweak measurements, the 14 Z-pole measurements and m_W in Table 2 and the 13 low-energy measurements in Table 3, we find

$$\left.\begin{aligned} m_t &= 160 \pm 11 \text{ GeV} \\ x_H &= -1.1^{+2.2}_{-1.1} \\ \delta_\alpha &= -0.02 \pm 0.35 \\ \alpha_s &= 0.120 \pm 0.003 \end{aligned}\right\} \quad \rho_{\text{corr}} = \begin{pmatrix} 1.0 & -0.5 & -0.8 & 0.2 \\ & 1.0 & 0.9 & -0.5 \\ & & 1.0 & -0.5 \\ & & & 1.0 \end{pmatrix}, \qquad 4.14.$$

where $\chi^2_{\text{min}}/(\text{d.o.f}) = 20.2/(28-4)$ (70% CL). It is remarkable that the resulting preferred values of m_t, δ_α, and α_s are all roughly consistent with their direct measurements (Equations 3.31, 2.22a, and 3.33). The preferred value of m_H is, however, rather small, barely consistent with the direct measurement bound (Equation 3.32). Here $x_H = \ln(m_H/100\,\text{GeV})$ in Equation 2.33.

By using our current knowledge to constrain α_s and δ_α, we can examine more closely the consistency between the m_t value extracted from the electroweak measurements and that of Equation 3.31. Table 5 shows the 1-σ allowed range of m_t and m_H.

Here we examine the dependences of the results on our choice of input electroweak data by excluding the A^0_{LR} data, or the b- and c-jet FB asymmetry data, or the R_b and R_c data. Remarkably, the preferred m_t range does not change much, and it is always slightly smaller than but consistent with the direct measurement (Equation 3.31). On the other hand, the preferred range of m_H is sensitive to the data choice for the first two cases. The removal of the A^0_{LR} data shifts the preferred m_H range up, while removal of the $A^{0,q}_{\text{FB}}$ data shifts the m_H range down to the excluded region. Figure 2 shows the fit results with some of the individual constraints (*a*) with all the electroweak data, (*b*) without the A^0_{LR} data, and (*c*) without the $A^{0,q}_{\text{FB}}$ data. It is the "asymmetry" band that changes significantly in the three cases. In (*a*) and (*b*), it is the data on R_ℓ and R_b (and also those from the low-energy data) that forbid the allowed m_t (and hence

Table 5 1-σ constraints on m_t and m_H in the minimal standard model

Data	m_t [GeV]	m_H [GeV]
EW, α_s[PDG], α[EJ]	160 ± 8	40^{+60}_{-20}
EW $- A^0_{LR}$, α_s[PDG], α[EJ]	161 ± 11	86^{+160}_{-47}
EW $- \{A^{0,b}_{FB}, A^{0,c}_{FB}\}$, α_s[PDG], α[EJ]	161 ± 7	24^{+26}_{-10}
EW $- \{R_b, R_c\}$, α_s[PDG], α[EJ]	163 ± 10	50^{+140}_{-25}

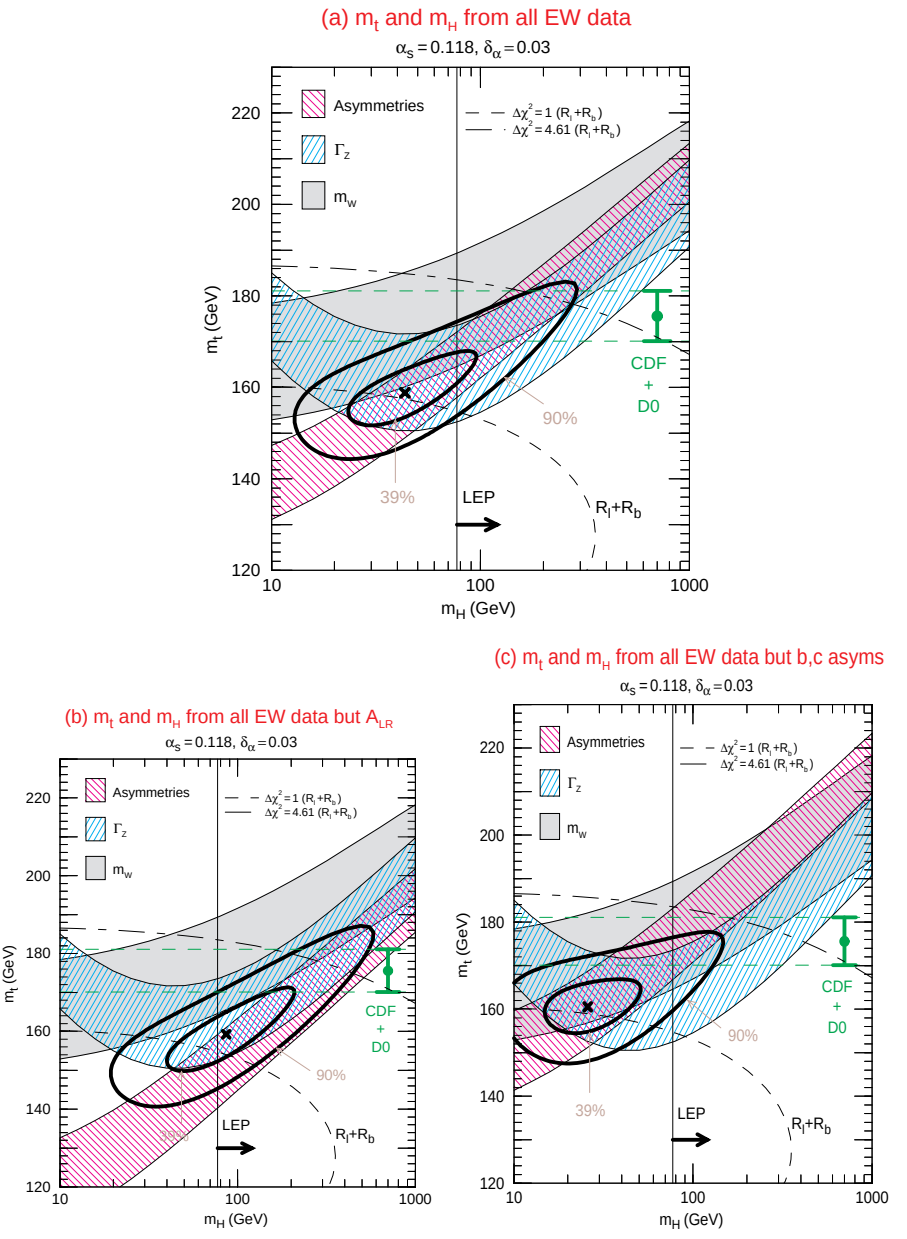

Figure 2 The standard-model fit to all electroweak data in the (m_H, m_t) plane. Thick inner and outer contours correspond to $\Delta\chi^2 = 1$ (~39% CL) and $\Delta\chi^2 = 4.61$ (~90% CL), respectively. The 1-σ bands from the Z-pole asymmetries, Γ_Z and m_W, are also shown. *Dashed lines* show constraints from R_ℓ and R_b. (*a*) is for all data, (*b*) without A_{LR}, and (*c*) without $A_{\rm FB}^{0,b}$ and $A_{\rm FB}^{0,c}$.

Table 6 90%-CL allowed range of m_H [GeV] in the minimal standard model

Data	90%-CL range [GeV]
EW, m_t, α[EJ]	$27 < m_H < 390$
EW, m_t, α_s [PDG], α[EJ]	$27 < m_H < 350$
EW, m_t, α_s[PDG], α[MZ]	$60 < m_H < 440$
EW, m_t, α_s[PDG], α[DH]	$47 < m_H < 330$
EW $-\mathrm{A}^0_{LR}$, m_t,α_s[PDG], α [EJ]	$66 < m_H < 560$
EW $-\{\mathrm{A}^{0,b}_{FB}, A^{0,c}_{FB},\}$, m_t,α_s [PDG], α[EJ]	$9 < m_H < 220$
EW $-\{R_b, R_c\}$, m_t, α_s [PDG], α[EJ]	$31 < m_H < 400$

m_H) range to move up. In (*c*), the three shown bands force both m_t and m_H to be small. These exercises demonstrate that we do not find a consistent picture by removing the part of the data that gives a high "pull" in Table 2.

Table 6 shows the 90%-CL allowed range of m_H by taking into account the m_t data (Equation 3.31). The variation that results from the three estimates of δ_α, Equation 2.22, is also shown. Since at present the conservative estimate of Equation 2.22a is consistent with both Equations 2.22b and 2.22c, which rely on perturbative QCD at low energies, we cannot make a definite statement about the upper bound on m_H. It is probably fair to say that the 95%-CL upper limit on m_H is somewhere between 300 GeV and 450 GeV from the electroweak measurements in the minimal standard model. For reference, the table also shows cases in which part of the data are removed in the fit.

4.4 *Implications for Physics beyond the Standard Model*

The above study shows that the electroweak data are consistent with the minimal standard model, with some preference for m_H smaller than a few hundred GeV. This observation may lead to a constraint on physics beyond the standard model. We examine here briefly several examples.

4.4.1 SUPERSYMMETRIC STANDARD MODEL The supersymmetric extension of the standard model, SUSY-SM, is the favorite solution to the gauge hierarchy problem (56), which is to say the smallness of the Higgs vev squared in units of the grand unified theory (GUT) scale of $\sim 10^{32}$ GeV^2, the scale at which the strong, weak, and electromagnetic interactions unify (57). Theorists have taken this hierarchy problem seriously because unified theories provide an elegant explanation of the quantization of electric charges (58). Supersymmetry, the symmetry between the fermionic and bosonic fields, solves the problem by pairing the Higgs bosons with fermionic partners (59). Even though supersymmetry is broken, the masses of the Higgs bosons and the superpartners of

quarks, leptons, and gauge bosons can be naturally arranged to vary only logarithmically with the energy scale (60), just as the gauge couplings do. It is even possible that the large top-quark Yukawa coupling induces the spontaneous breaking of the $SU(2)_L \otimes U(1)_Y$ symmetry (61).

These models, especially the minimal supersymmetric standard model (MSSM) with just a pair of Higgs doublets, have received serious phenomenological attention because the $SU(2)_L$ and $U(1)_Y$ gauge couplings determined by the electroweak measurements (see Equation 2.34) unify almost perfectly with the QCD coupling at 2×10^{16} GeV, if all the MSSM particles are present at or below the TeV scale (62).

The consequences of the supersymmetric standard model can be summarized as follows. When the masses of additional particles are all heavy, the models reduce to the minimal standard model, where m_H is bounded from above: $m_H \lesssim 130$ GeV in the MSSM (63), or $m_H \lesssim 150$ GeV (64) in a more general class of models that do not spoil coupling constant unification. If some of the additional particles have masses of order 100 GeV or less, then their effects could affect radiative corrections. They would contribute to $S_{\rm new}$, $T_{\rm new}$, and $U_{\rm new}$; to the difference $\overline{g}_Z^2(m_Z^2) - \overline{g}_Z^2(0)$ (Equation 2.28); to the μ-decay amplitude (Equation 2.26) as $[\delta_G]_{\rm new}$; and to the Z-decay amplitudes (Equation 3.9) as $[g_\alpha^f]_{\rm new}$. All these effects have been evaluated (65, 66), and no significant improvements over the standard model are found when the nonobservation of supersymmetric particles at the Tevatron and LEP2 is taken into account. Nevertheless, if relatively light superpartners exist, their effect could be detected via precision experiments. As an example, the dots in Figure 1 show the contribution of squarks and sleptons when one of their masses is below 200 GeV. Many but not all such scenarios are excluded by the present data because they predict too large a value of ΔT. The search for supersymmetric particles is clearly one of the most important tasks of high-energy physics.

4.4.2 TECHNICOLOR MODELS An alternative solution to the gauge-hierarchy problem is to discard the scalar boson from the standard model entirely and to obtain the electroweak symmetry-breaking vev as a consequence of a fermion-pair condensate, just as chiral symmetry is broken by the quark-antiquark condensate in QCD. The resulting pseudo-Goldstone bosons can make the W and Z bosons massive. These models are generally called technicolor models because their prototype (8) makes use of the similarity to QCD: In place of quarks are techniquarks, and in place of the color force is an even stronger technicolor force to make the condensate denser by a factor of $v/f_\pi \sim 2{,}000$.

In this class of models, if the dynamics is indeed similar to QCD, then there is a prediction for the S parameter. Using the notation

$$(S_{\rm PT}, T_{\rm PT}, U_{\rm PT}) \approx (\Delta S, \Delta T, \Delta U) - (\Delta S, \Delta T, \Delta U)_{\rm SM}^{[m_H = 1\ {\rm TeV}]}, \qquad 4.15.$$

Peskin & Takeuchi (22) found

$$S_{\rm PT} \approx 0.3\,\frac{N_{\rm TF}}{2}\,\frac{N_{\rm TC}}{3} > 0.2, \qquad 4.16.$$

where $N_{\rm TF} \geq 2$ is the number of technifermions and $N_{\rm TC} \geq 2$ is the number of colors. From the fit of Equations 4.11 and 4.12, we find for the estimates of Equations 2.22a, 3.33, 3.31

$$S_{\rm PT} = -0.25 + 20\left[g_L^b\right]_{\rm new} \pm 0.14, \qquad 4.17a.$$

$$T_{\rm PT} = 0.33 + 0.74\,S_{\rm PT} + 43\left[g_L^b\right]_{\rm new} \pm 0.11, \qquad 4.17b.$$

$$U_{\rm PT} = 0.62 + 0.84\,S_{\rm PT} - 1.24\,T_{\rm PT} \pm 0.27, \qquad 4.17c.$$

$$\left[g_L^b\right]_{\rm new} = -0.0015 \pm 0.0009, \qquad 4.17d.$$

with $\chi^2_{\rm min}/({\rm d.o.f}) = 18.6/24$. The prediction (Equation 4.16) is ruled out by the data (Equation 4.17a) by more than 3-σ.

Various modifications of the original idea have been proposed (67, 68), some of which give a negative value of $S_{\rm PT}$ consistent with Equation 4.17a. There remains the challenge of constructing a model in which the other three constraints in Equation 4.17 are satisfied and the flavor-changing processes are suppressed.

4.4.3 COMPOSITE MODELS Before the Z-pole experiments verified the predictions of the electroweak gauge theory, there were speculations that the weak bosons might be composite vector bosons like the ρ-mesons of QCD (69). In such theories, the vector-boson loop corrections do not have the universality that allows renormalization of the part of the quantum corrections that are sensitive to physics at very high energies. In gauge theories, the universality of all the gauge interactions leads to a universal high-energy behavior of the quantum corrections such that we can express our ignorance of physics at very high energies through a finite number of renormalization constants. The remaining finite quantum corrections can then tell us about particles with masses around the electroweak scale. The success of the electroweak theory, including the radiative effects, is a clear demonstration of the universality of the gauge interactions at energies beyond the top-quark–mass scale. Moreover, the attractive scenario of unification of the three gauge couplings applies only if the weak bosons are gauge bosons. Little motivation remains if the weak bosons are composite.

Whether the weak bosons are gauge bosons or merely behave like gauge bosons up to an energy scale far beyond the top-quark mass, it is possible that quarks and leptons are composite objects at a high energy scale. Remnants of the interactions that bind quarks and leptons may then appear as dimension-six contact interactions between a pair of fermionic currents. They can be

parameterized as (70)

$$\mathcal{L}_{\rm NC} = \sum_{f,f'} \sum_{\alpha,\beta} \eta^{ff'}_{\alpha\beta} (\bar{\psi}_f \gamma^\mu P_\alpha \psi_f)(\bar{\psi}_{f'} \gamma_\mu P_\beta \psi_{f'}), \qquad 4.18.$$

for neutral currents. Such new interactions modify our reduced amplitudes (Equation 3.3) as

$$M^{ff'}_{\alpha\beta}(q^2) = M^{ff'}_{\alpha\beta}(q^2)_{\rm SM} + \eta^{ff'}_{\alpha\beta}. \qquad 4.19.$$

Such a modification does not alter significantly the Z-pole measurements but affects low-energy observables of Table 3. Comprehensive studies of constraints on various contact interactions (41) are found to be competitive with experiments at high-energy colliders (71).

4.4.4 MODELS WITH NONDOUBLET HIGGS BOSONS The electroweak prediction of m_t based on the assumption of Equation 2.15 agrees well with its observed value (Equation 3.31), strongly suggesting that the Higgs bosons that give masses to W and Z are the doublets that give masses to quarks and leptons. This observation can be quantified by obtaining the constraint on the new-physics contribution to the T parameter, using all the data while allowing m_H to vary freely in the range 77 GeV $< m_H <$ 1 TeV. We find the 95%-CL lower and upper limits to be (72)

$$-0.0018 < \alpha T_{\rm new} < 0.0034. \qquad 4.20.$$

We can interpret this result as the constraint on the nondoublet Higgs-boson contribution, Equation 2.16. As an example, if there are $|Y_i| = 1$ and $Y_i = 0$ Higgs triplets, and the sum of their squared vevs is $v^2_{(1,1)}$ and $v^2_{(1,0)}$, respectively, then the constraint reads

$$-0.0018 < \frac{4v^2_{(1,0)} - 2v^2_{(1,1)}}{v^2} < 0.0034. \qquad 4.21.$$

Either $v^2_{(1,Y)}/v^2 \sim 0.001$ or subtle cancellation should take place. The Higgs-doublet origin of the weak-boson masses is among the most important information to emerge from the precision experiments.

It is worth noting that Equation 4.20 can also be interpreted as the constraint on the new-physics contribution to the charged-current interactions in μ-decay (72). Along with the universality of quark and lepton charged currents, that constraint is expressed in the unitarity of the Cabibbo-Kobayashi-Maskawa matrix (9)

$$|V_{ud}|^2 + |V_{us}|^2 + |V_{ub}|^2 = 0.9965 \pm 0.0021. \qquad 4.22.$$

One can also obtain constraints on the charged-current interactions between quarks and leptons (72, 73).

4.4.5 MODELS WITH EXTRA GAUGE BOSONS The limits on contact interactions (Equation 4.18) can be interpreted (41) as limits on the additional weak bosons, e.g. through the identity

$$\eta_{\alpha\beta}^{ff'} = -\frac{g_\alpha^f g_\beta^{f'}}{m_{Z_E}^2}, \qquad 4.23.$$

where the g_α^f are the Z_E couplings to the f_α current. Constraints on the mass of the extra Z-boson from the low-energy measurements of Table 3 have been determined (41) for the Z_E models within the E_6 unified theory.

Severe constraints on the Z_E boson are also found if it mixes significantly with the standard-model Z boson. A comprehensive study of the constraints on the Z_E models (74) has recently been repeated (76) by allowing for an arbitrary kinetic mixing term δ between Z_E and the hypercharge boson B (75). The 95%-CL lower mass bound of the Z_E-boson mass exceeds 1 TeV (for $g_E = g_Y$) in all the E_6 models studied if

$$\left| \frac{g_Z}{g_E} \frac{m_{ZZ'}^2}{m_Z^2} - \delta \right| \gtrsim 0.1. \qquad 4.24.$$

The left-hand side of the above inequality can be calculated in a given model, so the precision measurements constrain significantly the models with an extra Z boson if its mass is below 1 TeV. On the other hand, if the Z'-boson mass exceeds 1 TeV, we may encounter another mini-hierarchy problem even in supersymmetric models (74, 77).

5. SUMMARY AND OUTLOOK

After the completion of the LEP1 and SLC experiments, we may summarize our knowledge as follows:

1. The universality of the Z-boson interactions with quarks and leptons has been established with high precision.

2. The predictive power of the renormalizable electroweak theory has been established as the allowed top-quark–mass range in the electroweak analysis, $m_t = 160 \pm 8$ GeV, agrees well with the direct observation, $m_t = 175.6 \pm 5.5$ GeV, at the Tevatron.

3. The above agreement implies that the physics responsible for breaking the $SU(2)_L \otimes U(1)_Y$ gauge symmetry should respect the global SU(2) symmetry under which the triplet of the $SU(2)_L$ gauge bosons, W^1, W^2, and W^3,

acquire the same mass. Severe constraints are hence found for nondoublet nonsinglet Higgs-boson vevs.

4. The simplest mechanism for electroweak symmetry breaking, the minimal standard model, in which an $SU(2)_L$ doublet of the Higgs boson gives masses to the weak bosons as well as all the quarks and leptons, accommodates the data well if the Higgs-boson mass lies in the range $77\ \text{GeV} < m_H \lesssim 400\ \text{GeV}$.

5. If electroweak symmetry is broken by new strong interactions, then the theory should accommodate not only the constraint $S_{\text{PT}} = -0.25 \pm 0.14$ but also two additional ones among S_{PT}, T_{PT}, and U_{PT} (see Equation 4.17).

6. The observed effective weak mixing angle $\sin^2\theta_W$ at the m_Z scale allows unification of all three gauge couplings at the scale 2×10^{16} GeV if the particle spectrum at the weak scale ($\lesssim$1 TeV) is that of the MSSM.

7. The radiative corrections to electroweak observables in the MSSM do not differ much from those in the minimal standard model with a light Higgs boson ($m_H \lesssim 150$ GeV), unless certain new particle masses lie very near the minimum values allowed by direct search experiments.

8. Stringent constraints arise for new gauge interactions if the new weak bosons mix significantly with the standard Z boson.

In conclusion, precision measurements at the Z-pole contributed decisively to establishing the gauge theory of the electroweak interactions. The data have been presented in such a way that they will continue to be useful in the future, when more accurate information on m_t, $\alpha_s(m_Z)$, $\bar{\alpha}(m_Z^2)$, and higher-order radiative corrections is available. The data constrained the elusive Higgs sector of the electroweak theory and will constrain new physics once the Higgs boson is found. Further improvements are expected for the left-right asymmetry from SLC, the m_W measurements at LEP2 and the Tevatron, and the m_t measurements at the Tevatron, as well as possibly for the FB asymmetry of the leptonic decays of the Z bosons produced at the Tevatron or LHC. With the LEP1 data, these new measurements will shed light on physics beyond the standard model.

ACKNOWLEDGMENTS

The author wishes to thank S Matsumoto, GC Cho, and Y Umeda for collaboration that contributed much to the present report. He also thanks D Schaile for discussions and encouragement.

Literature Cited

1. Higgs PW. *Phys. Lett.* 12:132 (1964); *Phys. Rev.* 145:1156(1966)
2. Weinberg S. *Phys. Rev. Lett.* 19:1264 (1967)
3. Salam A. *Proc. 8th Nobel Symp.*, ed. N Svartholm, p. 367. Stockholm: Almqvist & Wiksell (1968)
4. Glashow SL. *Nucl. Phys.* 22:579 (1961)
5. 't Hooft G. *Nucl. Phys. B* 33:173 (1971); *Nucl. Phys. B* 35:167 (1971)
6. Glashow SL, Iliopoulos J, Maiani L. *Phys. Rev. D* 2:1285 (1970)
7. Veltman M. *Nucl. Phys. B* 123:89 (1977); Einhorn MB, Jones DRT, Veltman M. *Nucl. Phys. B* 191:146 (1981)
8. Weinberg S. *Phys. Rev. D* 19:1277 (1979); Susskind L. *Phys. Rev. D* 20:2619 (1979)
9. Barnett RM, et al (Particle Data Group). *Phys. Rev. D* 54:1 (1996)
10. Gell-Mann M, Low FE. *Phys. Rev.* 95:1300 (1954)
11. Martin AD, Zeppenfeld D. *Phys. Lett. B* 345:558 (1995)
12. Swartz ML. *Phys. Rev. D* 53:5268 (1995)
13. Eidelman S, Jegerlehner F. *Z Phys. C* 67: 602 (1995)
14. Burkhardt H, Pietrzyk B. *Phys. Lett. B* 356:398 (1995)
15. Davier M, Hoycker A. hep-ph/9801361
16. Kühn JH, Steinhauser M. hep-ph/9802241
17. Hagiwara K, Haidt D, Kim CS, Matsumoto S. *Z Phys. C* 64:559 (1994); *Z Phys. C* 68:352(E) (1995)
18. Kennedy DC, Lynn BW. *Nucl. Phys. B* 322:1 (1989)
19. Cornwall JM, Papavassiliou J. *Phys. Rev. D* 40:3474 (1989); Degrassi G, Sirlin A. *Nucl. Phys. B* 383:73 (1992); *Phys. Rev. D* 46:3104 (1992); Degrassi G, Kniehl B, Sirlin A. *Phys. Rev. D* 48:R3963 (1993)
20. Hagiwara K, Matsumoto S, Szalapski R. *Phys. Lett. B* 357:411 (1995)
21. Papavassiliou J, de Rafael E, Watson NJ. *Nucl. Phys. B* 503:79 (1997)
22. Peskin ME, Takeuchi T. *Phys. Rev. Lett.* 65:964 (1990); *Phys. Rev. D* 46:381 (1992)
23. Holdom B, Terning J. *Phys. Lett. B* 247:88 (1990)
24. Marciano WJ, Rosner JL. *Phys. Rev. Lett.* 65:2963 (1990); *Phys. Rev. Lett.* 68:898(E) (1992)
25. Kennedy DC, Langacker P. *Phys. Rev. Lett.* 65:2967 (1990); *Phys. Rev. D* 44:1591 (1991)
26. Altarelli G, Barbieri R. *Phys. Lett. B* 253: 161 (1991); Altarelli G, Barbieri R, Jadach S. *Nucl. Phys. B* 369:3 (1992); Altarelli G, Barbieri R, Caravaglios F. *Nucl. Phys. B* 405:3 (1993); *Phys. Lett. B* 349:145 (1995)
27. Sirlin A. *Phys. Rev. D* 22:971 (1980)
28. Hagiwara K, Haidt D, Matsumoto S. *Eur. Phys. J. C* 2:95 (1998)
29. Bardin D, Hollik W, Passarino G, eds. Precision Calculation for *Z* Resonance CERN 95-03 (1995)
30. Degrassi G, Gambino P, Vicini A. *Phys. Lett. B* 383:219 (1996); Degrassi G, Gambino P, Sirlin A. *Phys. Lett. B* 394:188 (1997); Degrassi G, Gambino P, Passera M, Sirlin A. *Phys. Lett. B* 418:209 (1998)
31. Chetyrkin KG, Kühn JH, Steinhauser M. *Phys. Lett. B* 351:331 (1995); Avdeev L, Fleischer J, Mikhailov S, Tarasov O. *Phys. Lett. B* 336:560 (1994); *Phys. Lett. B* 349:597(E) (1995)
32. Czarnecki A, Kühn JH. *Phys. Rev. Lett.* 77:3955 (1996); Harlander R, Seidensticker T, Steinhauser M. hep-ph/9712228
33. LEP Collaborations ALEPH, DELPHI, L3, OPAL, LEP Electroweak Work. Group and SLD Heavy Flavor Group. CERN-PPE/97-154
34. Altarelli G, Kleiss R, Verzegnassi C, eds. *Z Phys. at LEP1*. CERN 89-08 (1989)
35. LEP Heavy Flavor Group. LEPHF/97-01
36. Kim YK. Presented at Lepton-Photon Symp., Hamburg, 1997
37. Raja R. Presented at Recontres de Moriond, XXXIInd, Les Arcs, 1997
38. Janot P. Presented at Int. Europhys. Conf. High Energy Phys. (EPS97), Jerusalem, 1997
39. Kim JE, Langacker P, Levine M, Williams HH. *Rev. Mod. Phys.* 53:211 (1981)
40. Hewett JL, Takeuchi T, Thomas S. *Electroweak Symmetry Breaking and Beyond the Standard Model*. T Barklow, et al, eds. Singapore: World Sci. In press. hep-ph/9603391
41. Cho GC, Hagiwara K, Matsumoto S. *Eur. Phys. J. C* 5:155 (1998). hep-ph/9707334
42. Prescott CY, et al. *Phys. Lett. B* 84:524 (1979)
43. Argento A, et al. *Phys. Lett. B* 120:245 (1983)
44. Souder PA, et al. *Phys. Rev. Lett.* 65:694 (1990)
45. Heil W, et al. *Nucl. Phys. B* 327:1 (1989)
46. Blundell SA, Sapirstein J, Johnson WR. *Phys. Rev. D* 45:1602 (1992)
47. Marciano WJ, Sirlin A. *Phys. Rev. D* 27: 552 (1983); 29:75 (1984)
48. Noecker MC, Masterson BP, Wieman CE. *Phys. Rev. Lett.* 61:310 (1988)
49. Wood CS, et al. *Science* 275:1759 (1997)

50. Vetter PA, et al. *Phys. Rev. Lett.* 74:2658 (1995)
51. Edwards NH et al. *Phys. Rev. Lett.* 74:2654 (1995)
52. Rosner JL. *Phys. Rev. D* 53:2724 (1996); *Comments Nucl. Part. Phys. A* 22:205 (1998)
53. Fogli GL, Haidt D. *Z Phys. C* 40:379 (1988)
54. McFarland K, et al. *Eur. Phys. J. C* 1:509 (1998)
55. CHARM-II Collaboration. *Phys. Lett. B* 281:159 (1992)
56. Gildner E, Weinberg S. *Phys. Rev. D* 13:1333 (1976); Gildner E. *Phys. Rev. D* 14:1667 (1976)
57. Georgi H, Quinn HR, Weinberg S. *Phys. Rev. Lett.* 33:451 (1974)
58. Georgi H, Glashow SL. *Phys. Rev. Lett.* 32:438 (1974)
59. Witten E. *Nucl. Phys. B* 188:513 (1981); Dimopoulos S, Georgi H. *Nucl. Phys. B* 193:150 (1981); Sakai N. *Z Phys. C* 11:153 (1981)
60. Inoue K, Kakuto A, Komatsu H, Takeshita S. *Prog. Theor. Phys.* 68:927 (1992); *Prog. Theor. Phys.* 70:300(E) (1983); *Prog. Theor. Phys.* 71:413 (1984)
61. Ibáñez LE, Ross GG. *Phys. Lett.* 110B:215 (1982); Ibáñez LE. *Phys. Lett.* 118B:72 (1982); Ellis J, Nanopoulos DV, Tamvakis K. *Phys. Lett.* 121B:123 (1983) ; Alvarez-Gaumé L, Polchinski J, Wise MB. *Nucl. Phys. B* 221:495 (1983)
62. Giunti C, Kim CW, Lee UW. *Mod. Phys. Lett. A* 6:1745 (1991); Amaldi U, de Boer W, Fürstenau H. *Phys. Lett. B* 260:447 (1991); Langacker P, Luo M. *Phys. Rev. D* 44:817 (1991); Ellis J, Kelley S, Nanopoulos DV. *Phys. Lett. B* 260:131 (1991)
63. Okada Y, Yamaguchi M, Yanagida T. *Prog. Theor. Phys.* 85:1 (1991); Haber H, Hempfling R. *Phys. Rev. Lett.* 66:1815 (1991); Ellis J, Ridorfi G, Zwirner F. *Phys. Lett. B* 257:83 (1991)
64. Kane GL, Kolda C, Wells JD. *Phys. Rev. Lett.* 70:2686 (1993); Comeli D, Verzegnassi C. *Phys. Rev. D* 47:764 (1993)
65. Barbieri R, Caravaglion F, Frigeni M. *Phys. Lett. B* 279:169 (1992); Altarelli G, Barbieri R, Caravaglios F, *Phys. Lett. B* 314:357 (1993); Chankowski PH, et al. *Nucl. Phys. B* 417:101 (1994); Chankowski P, Pokorski S. *Phys. Lett. B* 366:188 (1996); Brignole A, Faruglio F, Zwirner F. *Z Phys. C* 71:679 (1996)
66. Carena M, et al. *Nucl. Phys. B* 491:103 (1997); de Boer W, et al. *Z Phys. C* 75:627 (1997); Chankowski PH, Ellis J, Pokorski S. hep-ph/9712234; Erler J, Pierce DM. hep-ph/9801238
67. Appelquist T, Terning J. *Phys. Lett. B* 315:139 (1993); *Phys. Rev. D* 50:2116 (1994); Chivukula RS, Dugan MJ, Golden M, Simmons EH. *Annu. Rev. Nucl. Part. Sci.* 45:255 (1) (1995); Appelquist T, Terning J, Wijewardhana LCR. *Phys. Rev. Lett.* 79:2767 (1997)
68. Holdom B. *Phys. Rev. D* 54:721 (1996); 54:1068 (1996)
69. Bjorken JD. *Phys. Rev. D* 19:335 (1978); Hung PD, Sakurai JJ. *Nucl. Phys. B* 143:81 (1978)
70. Eichten E, Lane K, Peskin ME. *Phys. Rev. Lett.* 50:811 (1983)
71. Barger V, Cheung K, Hagiwara K, Zeppenfeld D. *Phys. Lett. B* 404:147 (1997); *Phys. Rev. D* 57:391 (1998)
72. Hagiwara K, Matsumoto S. *Phys. Lett. B.* 424, 362 (1998). hep-ph/9712260
73. Altarelli G, et al. *Nucl. Phys. B* 506:3 (1997)
74. Cvetič M, et al. *Phys. Rev. D* 56:2861 (1997); Cvetič M, Langacker P. hep-ph/9707451
75. Holdom B. *Phys. Lett. B* 166:196 (1986); *Phys. Lett. B* 259:329 (1991); del Aguila F, Cvetič M, Langacker P. *Phys. Rev. D* 52:37 (1995); Babu KS, Kolda C, March-Russell J, *Phys. Rev. D* 54:4635 (1996); hep-ph/9710441
76. Umeda Y, Cho GC, Hagiwara K. *Phys. Rev. D.* In press. hep-ph/9805447; Cho GC, Hagiwara K, Umeda Y. *Nucl. Phys. B.* In press hep-ph/9805448
77. Drees M, Falck NK, Glück M. *Phys. Lett. B* 167:187 (1986)
78. Dienes KR. *Phys. Rep.* 287:447 (1997). hep-th/9602045

Annual Review of Nuclear and Particle Science
Volume 48, 1998

CONTENTS